# A UTOMATIC
# D YNAMIC
# I NCREMENTAL
# N ONLINEAR
# A NALYSIS

## Theory and Modeling Guide

### Volume II: Thermal

ADINA 9.6 April 2020

ADINA R & D, Inc.

# ADINA
# Theory and Modeling Guide

## Volume II: ADINA Thermal

April 2020

ADINA R & D, Inc.
71 Elton Avenue
Watertown, MA 02472 USA

tel. (617) 926-5199
telefax (617) 926-0238
www.adina.com

April 2020 Printing
Printed in the USA

# Table of contents

# 1. Introduction

## 1.1 Objective of this manual

The objective of this manual is to give a concise summary and guide for study of the theoretical basis of the finite element computer program ADINA Thermal (ADINA-T and ADINA-TMC). ADINA-T is employed for analysis of heat transfer and field problems and ADINA-TMC is employed for analysis of coupled thermo-mechanical problems.

Since a large number of analysis options is available in these computer programs, a user might well be initially overwhelmed with the different analysis choices and the theoretical bases of the computer programs. A significant number of publications referred to in the text (books, papers and reports) describe in detail the finite element analysis procedures used in the programs. However, this literature is very comprehensive and frequently provides more detail than the user needs to consult for the effective use of ADINA-T and ADINA-TMC. Furthermore, it is important that a user can identify easily which publication should be studied if more information is desired on a specific analysis option.

The intent with this Theory and Modeling Guide is

- to provide a document that summarizes the methods and assumptions used in ADINA Heat Transfer

- to provide specific references that describe the finite element procedures in more detail.

Hence, this manual has been compiled to provide a bridge between the actual practical use of the ADINA system and the theory documented in various publications. Much reference is made to the book *Finite Element Procedures* (ref. KJB) and to other publications but we endeavored to be specific when referencing these publications so as to help the reader to find directly the relevant information.

ref. K.J. Bathe, *Finite Element Procedures, 2nd ed.*, Cambridge, MA: Klaus-Jürgen Bathe, 2014.

We intend to update this report as we continue our work on the ADINA system. If you have any suggestions regarding the material discussed in this manual, we would be glad to hear from you.

## 1.2 ADINA System documentation

At the time of printing of this manual, the following documents are available with the ADINA System:

**Installation Notes**
Describes the installation of the ADINA System on your computer. Depending on the platform, the appropriate installation notes in pdf format can be printed or downloaded from http://www.adina.com

**ADINA Handbook**
Written as a task-oriented desktop reference, the ADINA handbook helps users to quickly and effectively leverage ADINA's advanced geometric modeling, meshing, and visualization features.

**ADINA User Interface Command Reference Manual**

**Volume I: ADINA Solids & Structures Model Definition**

**Volume II: ADINA Thermal Model Definition**

**Volume III: ADINA CFD & FSI Model Definition**

**Volume IV: ADINA EM Model Definition**

**Volume V: Display Processing**

These documents describe the AUI command language. You use the AUI command language to write batch files for the AUI.

**ADINA Primer**
Tutorial for the ADINA User Interface, presenting a sequence

of worked examples which progressively instruct you how to effectively use the ADINA System.

**Theory and Modeling Guide**

**Volume I: ADINA Solids & Structures**

**Volume II: ADINA Thermal**

**Volume III: ADINA CFD & FSI**

**Volume IV: ADINA EM**

Provides a concise summary and guide for the theoretical basis of the analysis programs. The manuals also provide references to other publications which contain further information, but the detail contained in the manuals is usually sufficient for effective understanding and use of the programs.

**ADINA Verification Manual**
Presents solutions to problems which verify and demonstrate the usage of the ADINA System. Input files for these problems are distributed along with the ADINA System programs.

**ADINA-Nastran Interface Manual**
Describes the ADINA-AUI Nastran Interface. This guide is available as a pdf file. The Nastran Case Control Commands, Parameters, and Bulk Data Entries that are supported by the AUI are documented.

**TRANSOR for I-DEAS Users Guide**
Describes the interface between the ADINA System and NX I-deas. This guide is available in html format and is directly accessible from the TRANSOR interface within I-deas. The use of TRANSOR for I-deas to perform pre-/post-processing and ADINA analysis within the I-deas environment, is described.

**TRANSOR for Femap Users Guide**
Describes the interface between the ADINA System and Femap. This guide is available as a pdf file. The use of TRANSOR for Femap to perform pre-/post-processing and ADINA analysis

within the Femap environment, is described.

**ADINA System 9.6 Release Notes**
Provides a description of the new and modified features of the ADINA System 9.6.

# 2. Heat transfer equations

## 2.1 Governing equations

*ref. KJB Section 7.2.1*

- For heat transfer in a body, we assume that the material of the body obeys Fourier's law of heat conduction, i.e.,

$$q = -k\frac{\partial \theta}{\partial x}$$

where

$q$ = heat flux (heat flow conducted per unit area)
$\theta$ = temperature
$k$ = thermal conductivity (material property)

- The law states that the heat flux is proportional to the temperature gradient, the constant of proportionality being the thermal conductivity, $k$, of the material. The minus sign indicates the physical fact that a positive heat flux along direction '$x$' is given by a drop in temperature $\theta$ in that direction $\partial\theta/\partial x < 0$ .

Consider a three-dimensional solid body as shown in Fig. 2.1-1. In the principal axis directions $x$, $y$, and $z$ we have

$$q_x = -k_x\frac{\partial \theta}{\partial x}; \quad q_y = -k_y\frac{\partial \theta}{\partial y}; \quad q_z = -k_z\frac{\partial \theta}{\partial z}$$

where $q_x, q_y, q_z$ and $k_x, k_y, k_z$ are the heat fluxes and conductivities in the principal axis directions. Equilibrium of heat flow in the interior of the body thus gives

$$\frac{\partial}{\partial x}\left(k_x\frac{\partial \theta}{\partial x}\right)+\frac{\partial}{\partial y}\left(k_y\frac{\partial \theta}{\partial y}\right)+\frac{\partial}{\partial z}\left(k_z\frac{\partial \theta}{\partial z}\right) = -q^B \qquad (2.1\text{-}1)$$

where $q^B$ is the rate of heat generated per unit volume.

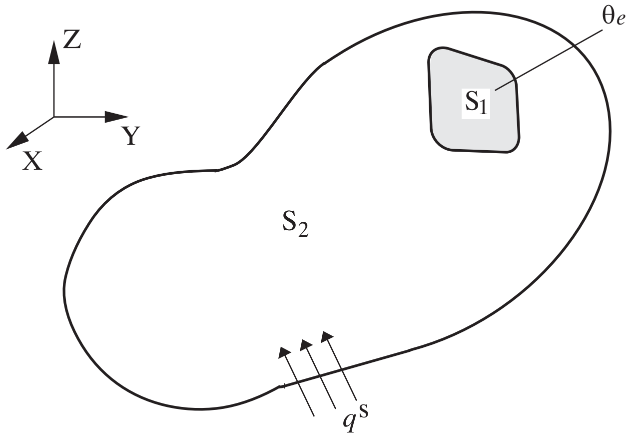


Figure 2.1-1: Body subject to heat transfer

Further details can be found in the following reference:

ref. Carslaw, H.S. and Jaeger, J.C., *Conduction of Heat in Solids*, 2nd ed., Oxford University Press, 1969.

- At the surfaces of the body the following conditions must be satisfied:

$$\theta\big|_{S_1} = \theta_e \tag{2.1-2}$$

$$k_n \frac{\partial \theta}{\partial n}\bigg|_{S_2} = q^S \tag{2.1-3}$$

$\theta_e$ is the external surface temperature (on surface $S_1$), $k_n$ is the body thermal conductivity in the direction $n$ of the outward normal to the surface, and $q^S$ is the heat flow input to the body across surface $S_2$.

- The governing principle of virtual temperatures corresponding to the above equation can be found in Section 7.2.1 of ref. KJB.

- Note that a time-dependent temperature distribution has not been considered in the above equations ─ i.e. steady-state conditions have been assumed. For transient problems the heat stored within the material is given by

$$q^C = C\dot{\theta} \tag{2.1-4}$$

where $C$ is the material heat capacity and the superposed dot denotes differentiation with respect to time. $q^C$ can be interpreted as forming part of the heat generation term $q^B$, i.e.,

$$q^B = \tilde{q}^B - C\dot{\theta} \tag{2.1-5}$$

where $\tilde{q}^B$ does not include any heat capacity effect.

## 2.2 Boundary and initial conditions

*ref. KJB Section 7.2.1*

- In heat transfer the following boundary conditions can be specified:

**Temperature conditions**: The temperature can be prescribed at specific points and surfaces of the body, denoted by $S_1$ in equation (2.1-2).

**Heat flow conditions**: The heat flow input can be prescribed at specific points and surfaces ($S_2$ in equation (2.1-3)).

**Convection boundary conditions**: Included in equation (2.1-3) are convection boundary conditions where

$$q^S = h\left(\theta_e - \theta^S\right) \tag{2.2-1}$$

with $h$ being the convection coefficient (possibly temperature dependent), $\theta_e$ the environmental (external) temperature, and $\theta^S$ the body surface temperature.

**Radiation boundary conditions**:  Also specified by equation (2.1-3) are the radiation boundary conditions

$$q^S = \kappa\left(\theta_r - \theta^S\right) \tag{2.2-2}$$

where $\theta_r$ is the temperature of the external radiation source, and $\kappa$ is the coefficient given by

$$\kappa = h_r\left(\theta_r^2 + \left(\theta^S\right)^2\right)\left(\theta_r + \theta^S\right) \tag{2.2-3}$$

where $h_r$ is determined from the Stefan-Boltzmann constant, the emissivity of the radiant and absorbing materials and the geometric view factors.

**Phase change**:  At a solid-liquid interface the latent heat is liberated (or absorbed) at a rate proportional to the volumetric rate of conversion of the material from one phase to the other.  This heat must also be balanced by the heat flow from (or to) the phase change "front".

The finite element equations are derived in the following reference:

ref. Rolph III, W.D. and Bathe, K.J., "An Efficient Algorithm for Analysis of Nonlinear Heat Transfer with Phase Changes", *Int. J. Num. Met. Eng*., Vol. 18, pp. 119-134, 1982.

**Initial conditions**:  For a transient analysis the temperature distribution at the start of the analysis must be specified.

## 2.3 Analogous field problems

*ref. KJB Section 7.3*

- The above equations for heat transfer analysis are also applicable to other field problems as summarized in Table 2.3-1. These analogies allow a heat transfer program to solve other field problems provided the analogous variables are utilized.

Table 2.3-1 Analogous field problems

| Problem | Variable $\theta$ | Constants $k_x, k_y, k_z$ | $q^B$ | $q^S$ |
|---|---|---|---|---|
| Heat transfer | Temperature | Thermal conductivity | Internal heat generation | Prescribed heat flow |
| Seepage | Total head | Permeability | Internal flow generation | Prescribed flow condition |
| Torsion | Stress function | 1/(Shear modulus) | 2* Angle of twist | — |
| Inviscid, incompressible irrotational flow | Potential function | 1 | Source/sink | Prescribed velocity |
| Electric conduction | Voltage | Electrical conductivity | Internal current source | Applied boundary current |
| Electrostatic field analysis | Field potential | Permittivity | Charge density | Prescribed field |

This page intentionally left blank.

# 3. Elements

This section gives further details on the formulation and discretization used by the elements available in ADINA-T.

## 3.1 1-D elements

- This simple element consists of two nodes, with only axial heat flow being transmitted, and has two degrees of freedom – the temperatures at each end of the element. A description of the element, including the local node numbering and the natural coordinate system, is given in Fig. 3.1-1 below.

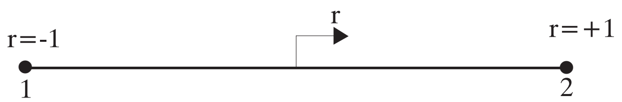


Figure 3.1-1: 1-D conduction element

- Linear interpolation functions are used for the geometry and the temperature.

- A one-point Gauss integration scheme is used to calculate all element matrices and vectors. The element requires one additional geometrical property, its cross-sectional area.

- This element can also be used as a radiation or convection link element. In such cases, the radiation or convection heat flow between two points in space is defined.

**Radiation link element:** The radiation heat flow in the link element is

$$Q = \sigma \varepsilon f A\left(\theta_1^4 - \theta_2^4\right)$$

where

$\sigma$ = Stefan-Boltzmann constant
$\varepsilon$ = emissivity (can be temperature dependent)

$f$ = shape factor
$A$ = area
$\theta_1, \theta_2$ = temperature at each end of the link

**Convection link element:** The convection heat flow in the link element is

$$Q = hA(\theta_1 - \theta_2)$$

where
$h$ = convection coefficient (can be temperature or time dependent)
$A$ = area
$\theta_1, \theta_2$ = temperature at each end of the link

## 3.2 2-D conduction elements

- The two-dimensional heat conduction elements available in ADINA-T can be planar or axisymmetric elements, as shown in Fig. 3.2-1.

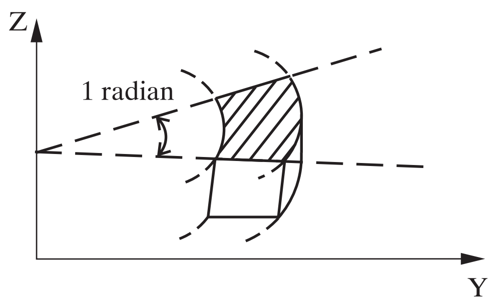


a) Axisymmetric finite element model (axisymmetric heat flow)

Figure 3.2-1: Axisymmetric and planar finite element models

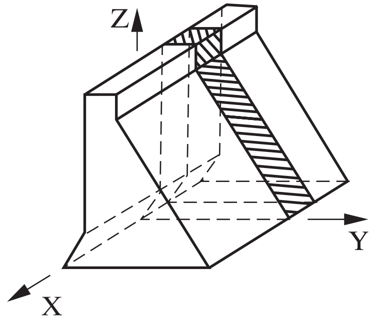


b) Planar finite element model (heat flow in YZ plane)

Figure 3.2-1: (continued)

- The elements are defined in the *YZ* plane, with the *Z* axis being the axis of rotational symmetry for axisymmetric elements. The *Y* axis represents the radial direction ($Y \geq 0$). Furthermore, the axisymmetric element models one radian of the physical domain. Thus when concentrated loads are applied to an axisymmetric element they must also refer to one radian.

- Fig. 3.2-2 shows the element nodal configurations supported by ADINA-T, and the element local node numbering and natural coordinate system. The recommended elements are the 8-node and 9-node parabolic quadrilateral elements, although linear 4-node quadrilateral and triangular degeneracies (by "collapsing" a side via coincident nodes as shown) are also possible.

- The element matrices are integrated numerically by Gauss integration; ADINA-T accepts integration orders (i.e., number of sampling points in each local coordinate direction) of 2, 3, or 4. The default order is 2, except for the 9-node element, for which the default integration order is 3.

- The planar 2-D conduction element requires one additional geometrical property, the element thickness (an axisymmetric element always extends one radian in the circumferential direction).

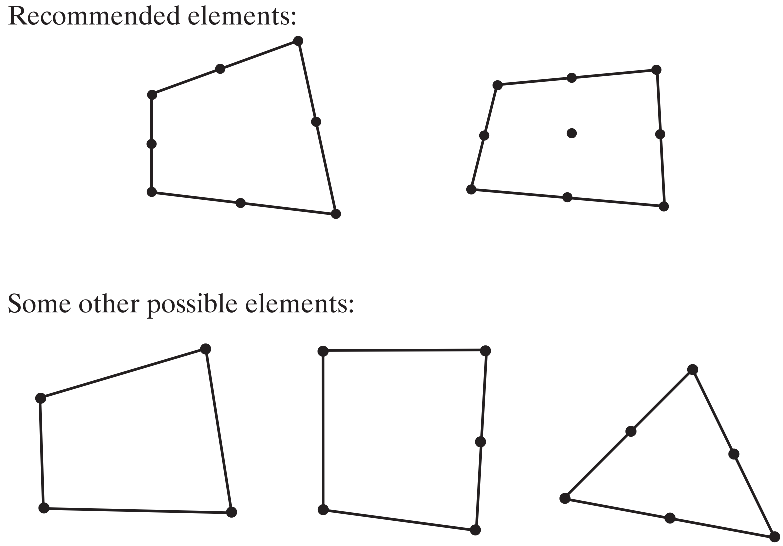


a) Typical nodal configurations

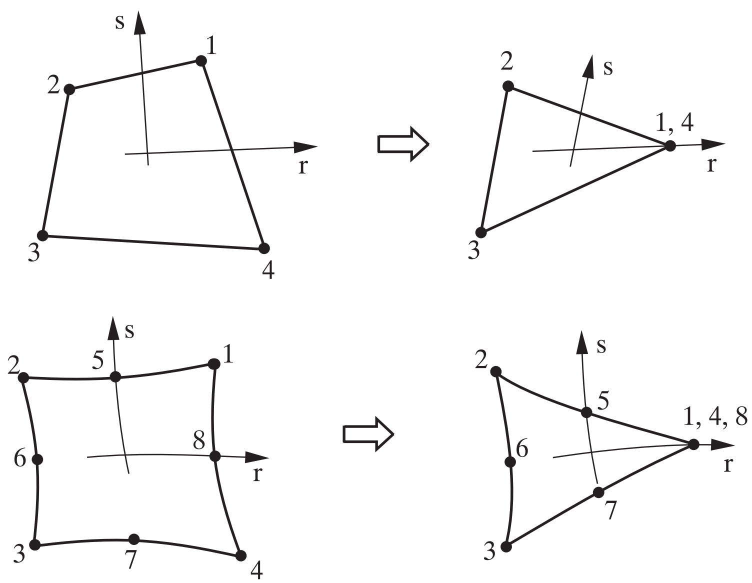


b) Degeneration of quadrilateral elements into triangular elements; local node numbering; natural coordinate system

Figure 3.2-2: 2-D conduction element

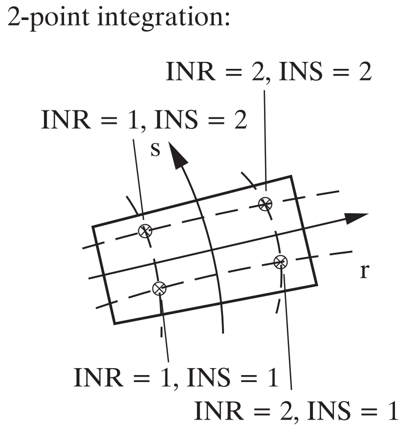


c) Element integration point labeling, INR=label number in r-direction, INS=label number in s-direction

Figure 3.2-2 (continued)

## 3.3 3-D conduction elements

- For general three-dimensional heat flow, ADINA-T provides hexahedral ("brick") elements with up to 27 nodes. The hexahedral elements can be degenerated into prismatic ("wedge") or tetrahedral elements by collapsing a face, or a face and edge respectively. The recommended elements, 20-node and 27-node hexahedral elements are illustrated in Fig. 3.3-1, along with other lower order and degenerate elements. The local node numbering convention and the integration point labeling are also given in the figure.

- The element matrices are integrated numerically by Gauss integration; ADINA-T accepts integration orders of 2, 3 or 4 in each local coordinate direction. The default order is 2 for elements with 20 or fewer nodes, or 3 for elements with more than 20 nodes.

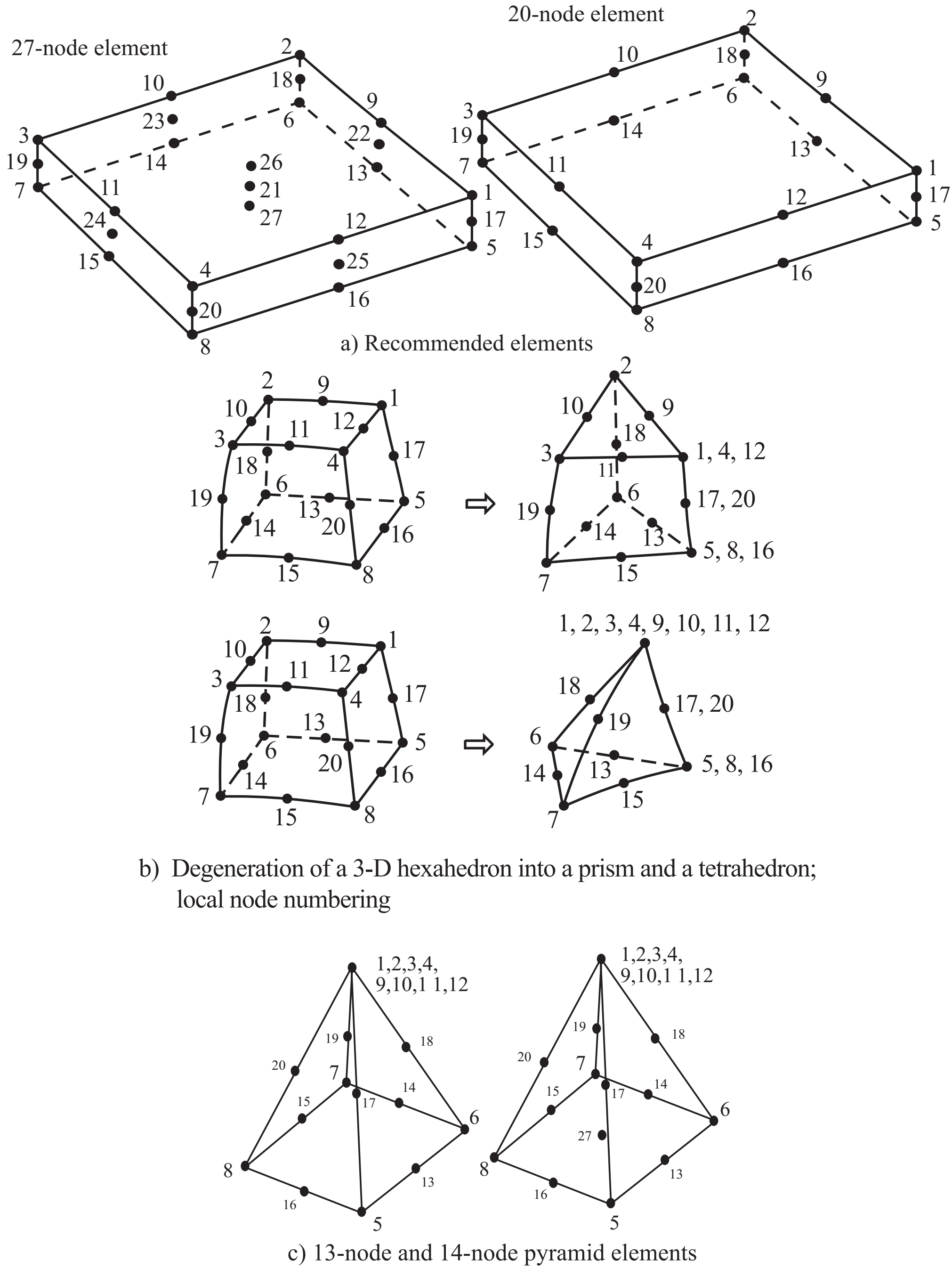


a) Recommended elements

b) Degeneration of a 3-D hexahedron into a prism and a tetrahedron; local node numbering

c) 13-node and 14-node pyramid elements

Figure 3.3-1: 3-D conduction element

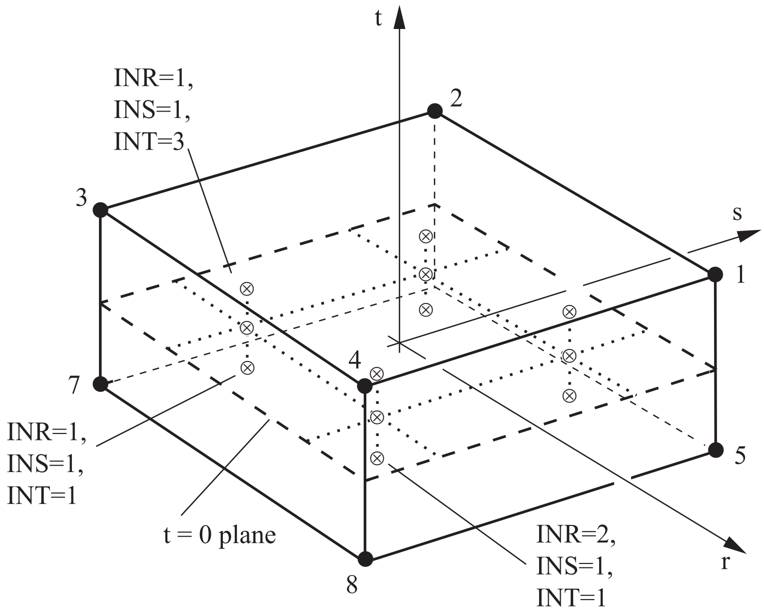


INR: label in r-direction; INS: label in s-direction; INT: label in t-direction

d) Integration point labeling; natural coordinate system

Figure 3.3-1 (continued)

## 3.4 Convection elements

- In ADINA-T boundary convection elements are used to specify the convection boundary condition

$$q^S = h\left(\theta_e - \theta^S\right)$$

where $h$ is the convection coefficient, $\theta_e$ is the external environment temperature, and $\theta^S$ is the unknown body surface temperature.

- The following types of boundary convection elements are available in ADINA-T (see Fig. 3.4-1):

**Node elements** with convection boundary conditions.

**Planar line elements** with convection boundary conditions, used in conjunction with 2-D conduction planar elements.

**Axisymmetric line elements** with convection boundary conditions, used in conjunction with 2-D conduction axisymmetric elements.

**Surface elements** with convection boundary conditions, used in conjunction with 3-D conduction or shell conduction elements.

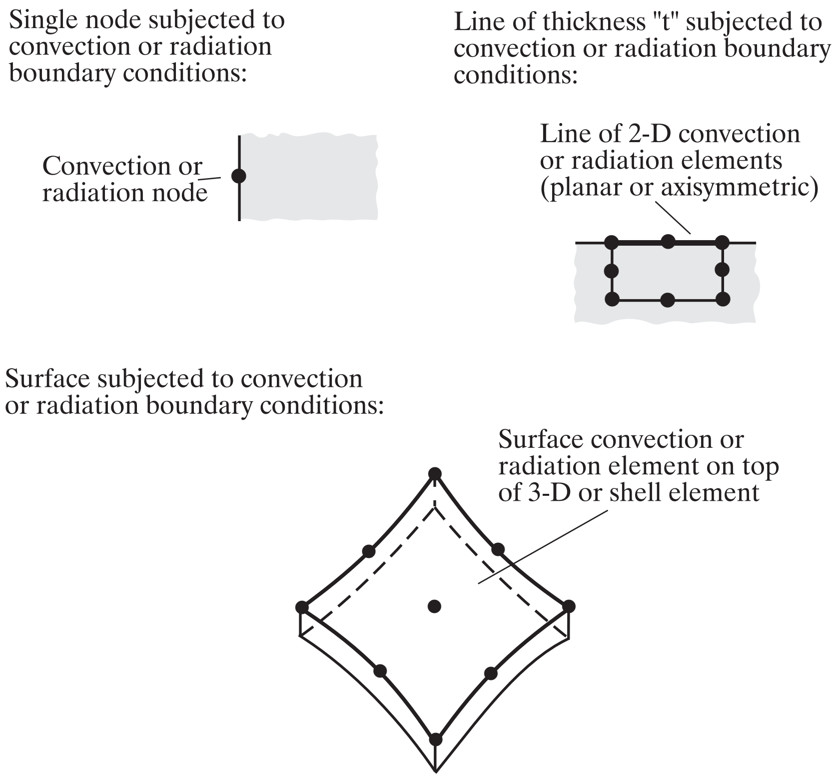


a) Convection or radiation element subtypes

Figure 3.4-1: Boundary convection or radiation elements

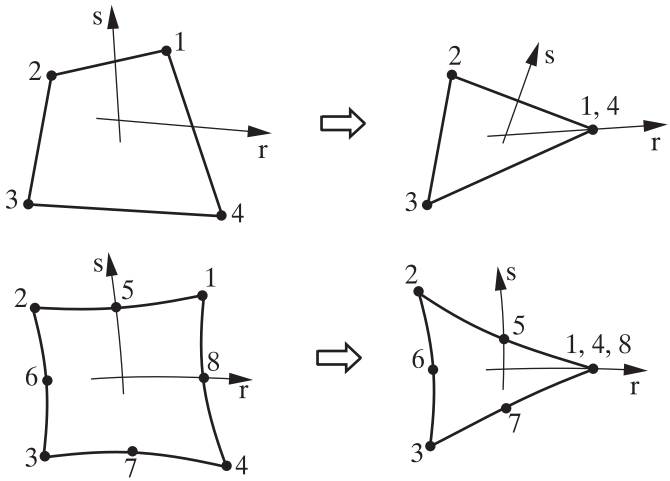


b) Degeneration of planar or axisymmetric convection or radiation elements; local node numbering; natural coordinate system

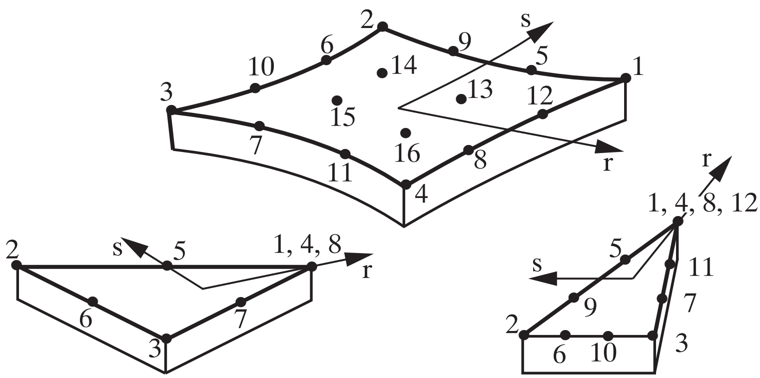


c) Degeneration of surface convection or radiation elements; local node numbering; natural coordinate system

Figure 3.4-1 (continued)

- The convection coefficient *h* can be constant, temperature-dependent, or time-dependent as specified by the material model of the boundary convection element group.

- The environmental temperature for each node can be specified via the convection load commands.

- The node convection element requires as an additional geometrical property a cross-sectional area, and the planar convection element requires a thickness in the direction normal to the plane of the element.

## 3.5 Radiation elements

- In ADINA-T, boundary radiation elements are used to specify the radiation boundary condition

$$q^S = \sigma f e\left(\theta_r^4 - \left(\theta^S\right)^4\right)$$

where $\sigma$ is the Stefan-Boltzmann constant, $f$ is a shape factor, $e$ is the material emissivity, $\theta_r$ is the temperature of the radiative source (or sink) and $\theta^S$ is the unknown body surface temperature.

- The following types of boundary radiation element are available in ADINA-T (see Fig. 3.4-1):

  **Node elements** with radiation boundary conditions

  **Planar line elements** with radiation boundary conditions, used in conjunction with 2-D conduction planar elements

  **Axisymmetric line elements** with radiation boundary conditions, used in conjunction with 2-D conduction axisymmetric elements

  **Surface elements** with radiation boundary conditions, used in conjunction with 3-D conduction or shell conduction elements.

The possible shapes of radiation elements, their local node numbering and natural coordinate system are identical to the boundary convection elements.

- The emissivity coefficient $e$ can be either constant or temperature-dependent and is specified, along with the Stefan-Boltzmann constant $\sigma$, in the material model of the boundary radiation element group.

- The radiative source/sink temperature $\theta_r$ for each node can be specified.

- The shape factor $f$ is input as an element physical property for all the radiation elements. In addition, the node element requires as input geometrical property a cross-sectional area, and the planar radiation element requires a line thickness normal to the plane of the element.

## 3.6 Shell conduction elements

- The shell conduction element is a 4- to 32-node isoparametric element that can be employed to model any shell structure (see Fig. 3.6-1).

- Node input options for transition elements: the interior nodes can only be employed for the rectangular fully parabolic element (9-node element with one interior node) and the rectangular fully cubic element (16-node element with four interior nodes).

- The same finite element model can be used for heat transfer analysis and later for stress analysis of a shell structure. However, if a thermal stress analysis is to be carried out, the selection of elements should be based on the structural behavior of the elements required for the stress analysis.

### 3.6.1 Element formulation

*ref KJB Section 5.4.2*

- The shell conduction element is formulated by treating the shell as a three-dimensional continuum assuming that the temperature varies linearly through the thickness direction.

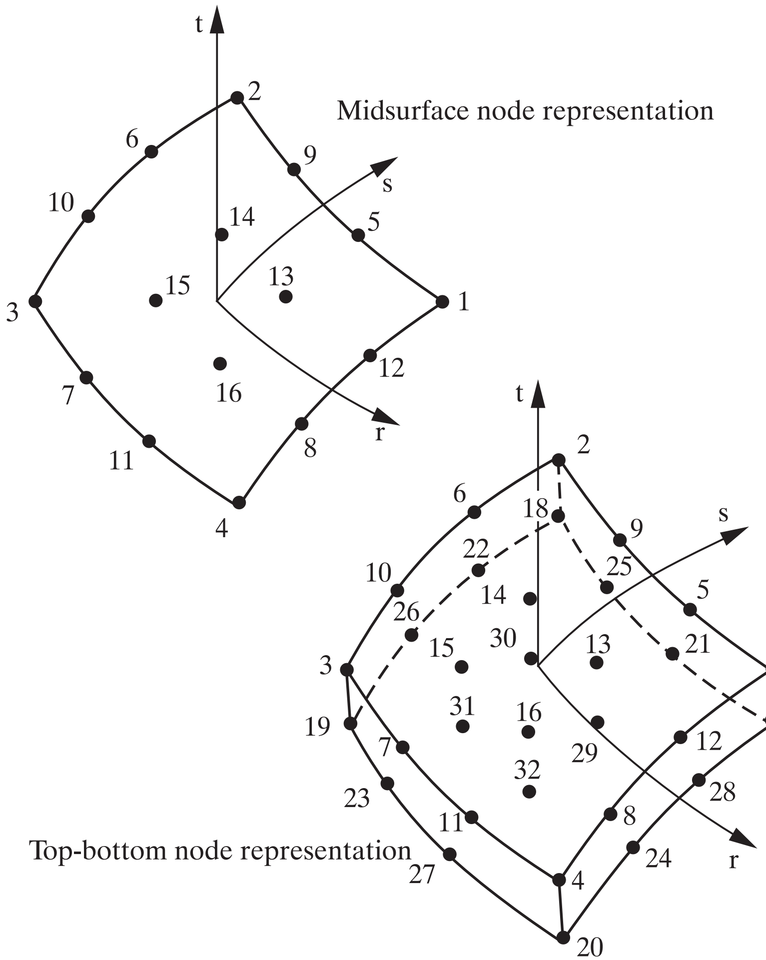


a) General shell conduction element

Figure 3.6-1: Shell conduction element configuration; local node numbering; natural coordinate system

Quadrilateral transition element: Triangular transition element:

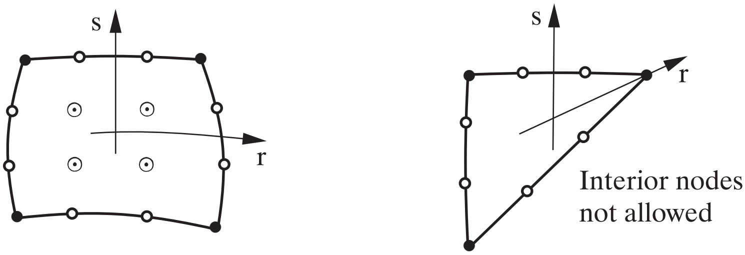


● Nodes or pairs of nodes
○ Optional nodes or pairs of nodes
⊙ Nodes allowed under special conditions

b) Special shell transition elements (not recommended for general use)

Figure 3.6-1 (continued)

- Based on the shell midsurface geometry, three-dimensional geometry is constructed, and nodes are assigned to the top and bottom face positions corresponding to the midsurface shell nodes.

- In the calculation of the three-dimensional geometry, the following geometric quantities are used

  - the coordinates of the node $k$ that lies on the shell element midsurface.

  - the director vector $\mathbf{V}_n^k$ normal to the shell midsurface.

  - the shell thickness, $a_k$, at the nodal points measured in the direction of the vector $\mathbf{V}_n^k$ (see Fig. 3.6-2)

- Fig. 3.6-2 shows a 4-node shell conduction element with the shell midsurface nodes, the nodal director vectors and constructed top and bottom nodes. The director vectors are automatically calculated by ADINA-T, see Fig. 3.6-3.

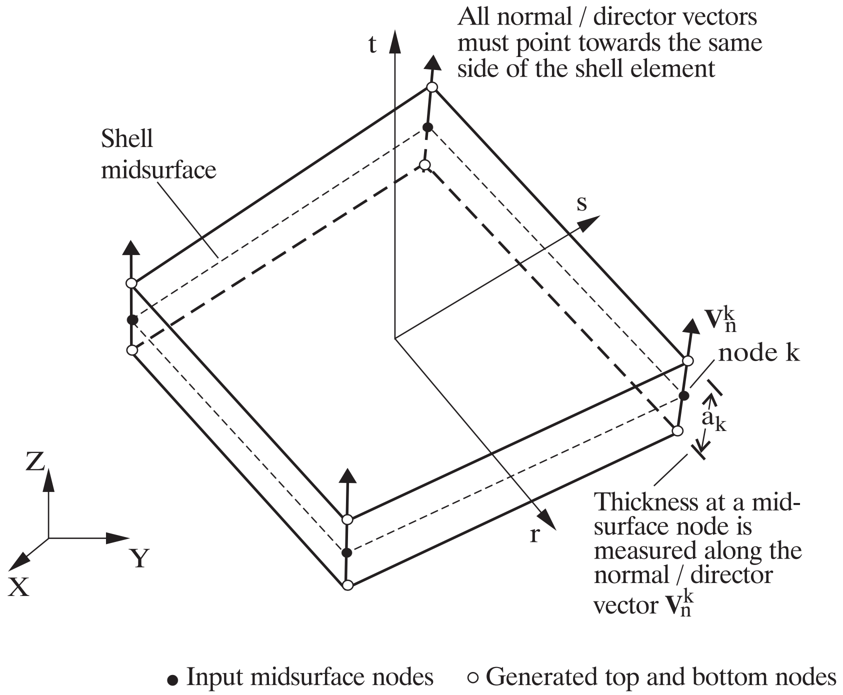


Figure 3.6-2: Description of the shell conduction element

- In the calculation of the shell element matrices, i.e., conductivity, heat capacity, heat generation and latent heat, the top and bottom nodes are used instead of midsurface nodes.

  Hence, an isoparametric formulation with three-dimensional interpolation functions is used.

- The shell heat capacity matrix can be calculated with a lumped or a consistent formulation. However, the lumped formulation must be used with the Euler forward time integration method.

- ADINA-T calculates temperatures for the top and bottom nodes, and then calculates temperatures and temperature gradients for the midsurface nodes. The nodal results are stored in the temperature and temperature gradient files for subsequent analysis with ADINA.

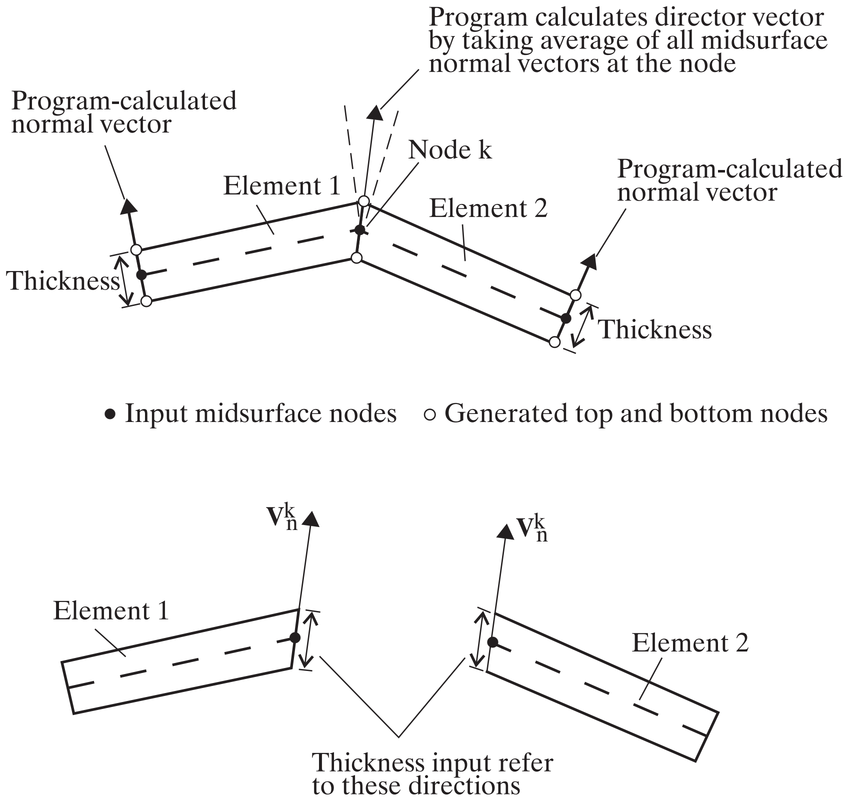


Figure 3.6-3: Program-calculated director vector at shell conduction element node

### 3.6.2 Transition elements

- The shell conduction elements can also be employed as transition elements. A transition element is defined by using, instead of a midsurface node, nodes on the top and bottom surfaces of the shell element. Fig. 3.6-4 shows a cubic transition element.

- The transition element is particularly useful in modeling shell to shell and shell to solid intersections, see Figs. 3.6-5 and 3.6-6.

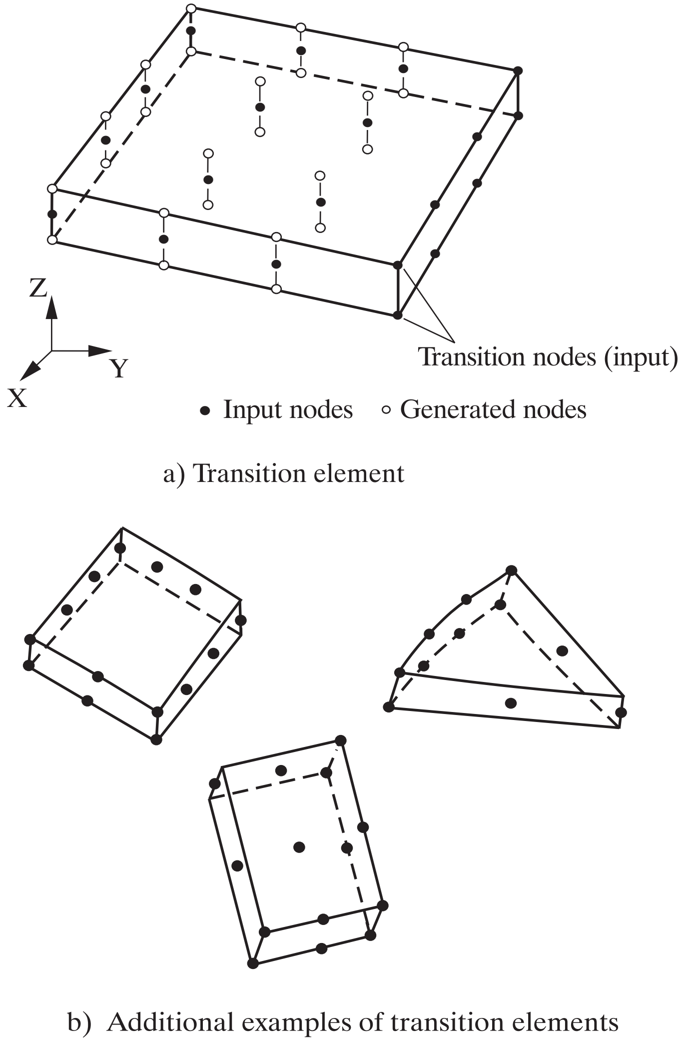


Figure 3.6-4: Shell conduction transition element

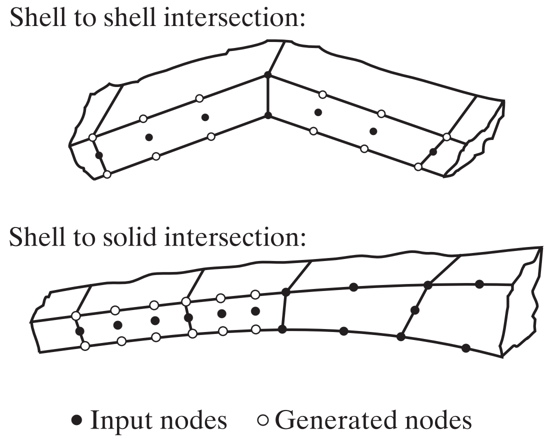


Figure 3.6-5: Examples of the use of shell conduction transition elements

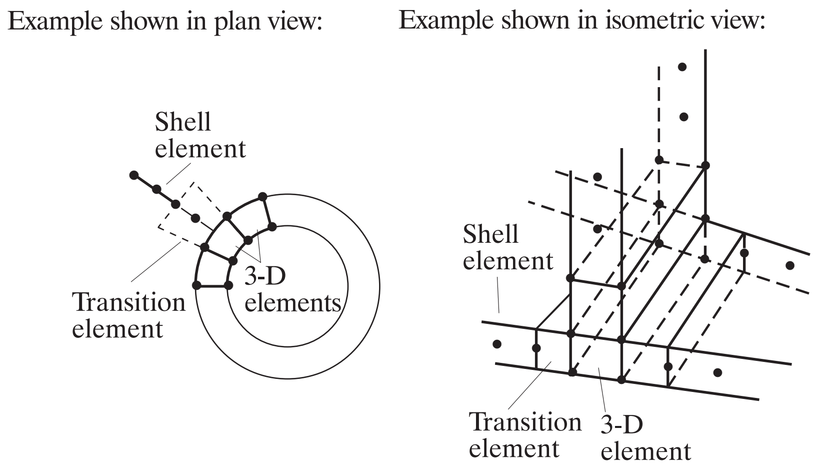


Figure 3.6-6: Examples of intersection modeling

### 3.6.3 Selection of elements for analysis

• The element selection should be based on the structural behavior of shell elements if the same geometry is to be used later for structural analysis.

- It is recommended that whenever possible, the 4-node, 8-node, or 16-node elements be employed.

- Numerical integration is used to evaluate the element matrices, and it is usually best to employ the default or a higher integration order.

- Gauss numerical integration is used in the r-s plane.  For the 4-node element shown in Fig. 3.6-7 (a), the default order is 2×2 point integration.  For the 8-node and 16-node elements in Fig. 3.6-7(b), (c), the default integrations are 3×3 and 4×4 point integration respectively.  Usually, 2-point Gauss integration through the shell thickness is appropriate for heat transfer analysis.  The shell conduction element integration point labeling is the same as in the 3-D conduction element (see Fig. 3.3-1).

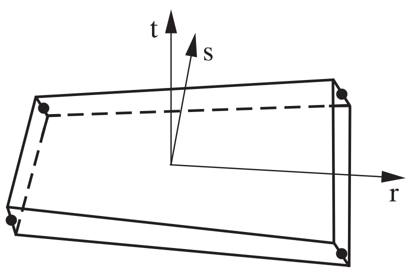


(a)  4-node shell element.  Use 2 × 2 Gauss integration in the r-s plane.

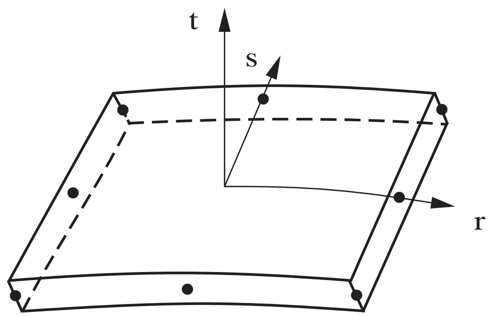


(b)  8-node shell element.  Use 3 × 3 Gauss integration in the r-s plane.

Figure 3.6-7:  Recommended elements for shell analysis

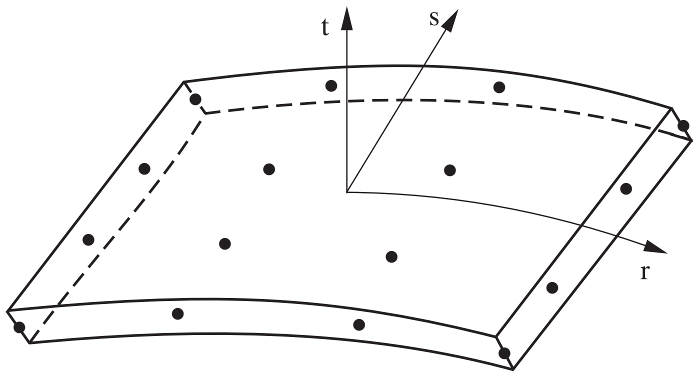


(c) 16-node cubic shell element. Use 4 × 4 Gauss integration in the r-s plane.

Figure 3.6-7 (continued)

This page intentionally left blank.

# 4. Material models

## 4.1 Constant material properties

### 4.1.1 Isotropic conductivity and heat capacity

- For this material model, thermal conductivity and heat capacity are independent of temperature and time and do not exhibit any directional dependence due to the material.

### 4.1.2 Orthotropic conductivity

- For this material model, thermal conductivity and heat capacity are independent of temperature and time. The thermal conductivity is orthotropic, that is, the model exhibits a directional dependency. Three constants $k_a, k_b, k_c$ give the thermal conductivity along the *a*-direction, *b*-direction, *c*-direction respectively. The *a-, b-* and *c-* material directions can be defined for each element.

- The heat capacity is isotropic for this model. The heat capacity is entered using the density $\rho$ and the specific heat per unit mass $c$. The product $\rho c$ is the specific heat per unit volume.

### 4.1.3 Seepage

- This material model defines the constants required for a seepage analysis. These are the permeability, $\tilde{k}$ and the weight density, $\gamma$, which are both isotropic and constant with respect to seepage head and time (see Fig. 4.1-1).

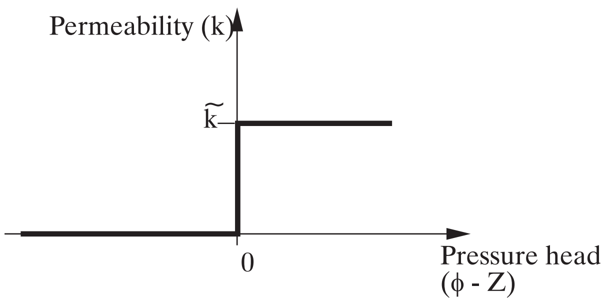


a) Material behavior

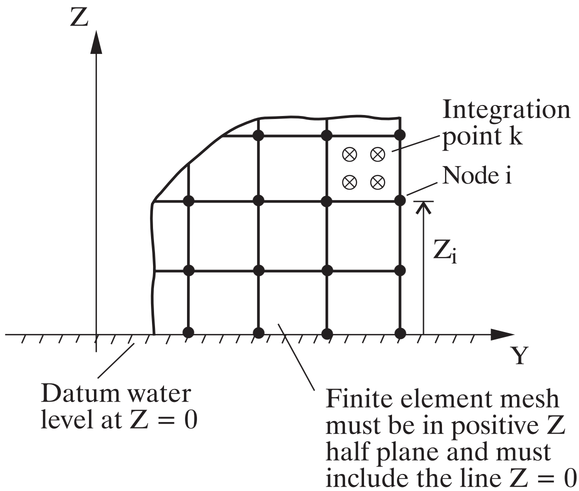


b) 2-D element modeling

Figure 4.1-1: Seepage analysis

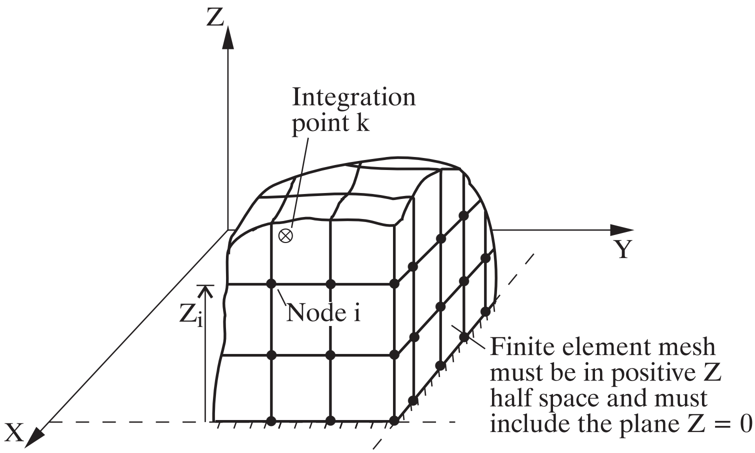


c) 3-D element modeling

Figure 4.1-1 (continued)

The Z coordinate at an integration point is computed using the nodal shape functions, i.e.

$$z_k = \sum_{i=1}^{n} h_i z^i$$

where $z_k$ is the Z-coordinate at integration point $k$, $h_i$ is the shape function for node $i$ (evaluated at integration point $k$) and $n$ is the number of nodes in the element.

### 4.1.4 Constant convection

- This material model specifies a temperature and time independent convection coefficient, for use with convection elements. The constant convection coefficient input, $h$, is used in the boundary condition

$$q^S = h\left(\theta_e - \theta^S\right)$$

where $\theta_e, \theta^S$ are the environmental and body surface temperatures respectively, and $q^S$ is the heat transfer due to surface convection.

### 4.1.5 Constant emissivity

- For this material model, a temperature and time independent emissivity coefficient is specified for use with radiation elements. The emissivity coefficient input, $e$ is used in the radiation boundary condition

$$q^r = \sigma f e\left[\theta_r^4 - \left(\theta^S\right)^4\right]$$

where $\sigma$ is the Stefan-Boltzmann constant, $f$ is the shape factor, $\theta_r$ is the temperature of the radiative source (or sink), $\theta^S$ is the body surface temperature and $q^r$ is the heat transfer due to surface radiation.

The emissivity $e$ and the Stefan-Boltzmann constant $\sigma$ must be input. Note: although $\sigma$ is a physical constant, it should be input with respect to the unit of temperature (Kelvin, Centigrade, Fahrenheit, or Rankine).

## 4.2 Temperature dependent material properties

- For these material models, some properties are functions of the temperature, and are defined using piecewise linear input curves.

### 4.2.1 Temperature dependent conductivity

- For this model, the thermal conductivity is isotropic and temperature dependent, i.e., $k = k(\theta)$ where $\theta$ is the temperature. The input is a table of $(\theta_i, k_i)$ values.

### 4.2.2 Temperature dependent heat capacity

- For this model, the heat capacity is isotropic and temperature dependent, i.e., $c = c(\theta)$ where $\theta$ is the temperature. The input is a table of $(\theta_i, c_i)$ values.

### 4.2.3 Temperature dependent heat capacity and constant orthotropic thermal conductivity

- For this material model, the thermal conductivity, $k$, is constant and orthotropic (see Section 4.1.2).

- The heat capacity is isotropic and temperature dependent (see Section 4.2.2).

### 4.2.4 Temperature dependent thermal conductivity and heat capacity

- For this material model, both the thermal conductivity and the heat capacity are isotropic and temperature dependent, i.e., $k = k(\theta)$, $c = c(\theta)$ where $\theta$ is the temperature.

### 4.2.5 Temperature dependent convection

- This material model specifies a temperature dependent convection coefficient (for use with convection elements). The coefficient, $h(\theta)$, is used in the boundary condition

$$q^S = h(\theta)\left(\theta_e - \theta^S\right)$$

where $\theta_e, \theta^S$ are the environmental and body surface temperatures respectively, and $q^S$ is the heat transfer due to surface convection. The dependence of $h$ on temperature can be specified as $h$ being either a function of $\theta^S$ or a function of the difference $\left(\theta_e - \theta^S\right)$. The input is a table of $\left(\theta_i, h_i\right)$ values.

### 4.2.6 Temperature dependent emissivity

- For this material model, a temperature dependent emissivity coefficient is input, i.e., $e = e(\theta)$ where $\theta$ is the temperature. The emissivity coefficient is used in the radiation boundary condition

$$q^r = \sigma f e\left[\theta_r^4 - \left(\theta^S\right)^4\right]$$

where $\sigma$ is the Stefan-Boltzmann constant, $f$ is the shape factor, $\theta_r$ is the temperature of the radiation source (or sink), $\theta^S$ is the body surface temperature, and $q^r$ is the heat transfer due to surface radiation.

The emissivity $e(\theta)$ is input as a table of ($\theta_i$, $e_i$) values. The Stefan-Boltzmann constant $\sigma$ is also an input value, which depends on the temperature unit (Kelvin, Centigrade, Fahrenheit, or Rankine).

# 4.3 Time dependent material properties

## 4.3.1 Time dependent thermal conductivity

- For this material model, the thermal conductivity is isotropic and time dependent, i.e., $k=k(t)$ where $t$ denotes time. The input is a table of $(t_i, k_i)$ values.

- The heat capacity is isotropic and constant.

## 4.3.2 Time dependent convection

- For this material model, the convection coefficient used in convection elements is specified to be time dependent, i.e., $h=h(t)$ where $t$ denotes time. The coefficient is used in the convection boundary condition

$$q^S = h(t)\left(\theta_e - \theta^S\right)$$

where $\theta_e, \theta^S$ are the environmental and body surface temperatures respectively, and $q^S$ is the heat transfer due to surface convection. The input is a table of $(t_i, h_i)$ values.

## 4.3.3 Condensation

- This material model defines time dependent condensation and convection coefficients. It can be used with convection elements when both condensation and convection heat transfer occur, e.g., in the modelling of steam turbines.

The following constants must be input:

$$T_{COND}, p_0, a, b, c, d, e, f, g$$

where $T_{COND}$, $p_0$, are the temperature and pressure respectively, below/above which condensation is not considered. Using these constants, the temperature of saturated steam is calculated by

$$\theta_e^{sat} = a + b\left(p\left(t\right)\right)^c \qquad p\left(t\right) \le d$$
$$e + f\left(p\left(t\right)\right)^g \qquad p\left(t\right) > d$$

$$0 < \theta_e^{sat} \le T_{COND}$$

where $p(t)$ is the time dependent pressure. The heat flow due to condensation is given by

$$q_{sat}^S = \alpha\left(t\right)\left(\theta_e^{sat} - \theta^S\right)$$

where $\theta^S$ is the body surface temperature, and that due to convection (of the superheated steam) is given by

$$q_{sup}^S = h\left(t\right)\left(\theta_e^{sup} - \theta^S\right)$$

where $\theta_e^{sup}$ is the steam temperature (which must be input).

- Condensation takes place when

$$q_{sat}^S > q_{sup}^S$$

and thus the actual heat flow, $q^S$ is given by

$$q^S = \begin{cases} \max\left(q_{sat}^S, q_{sup}^S\right) \text{ if } & \theta_e^{sat} \le T_{COND} \text{ and } p\left(t\right) \ge p_0 \\ q_{sup}^S \qquad \text{ if } & \theta_e^{sat} > T_{COND} \text{ or } p\left(t\right) < p_0 \end{cases}$$

But, if the sign of $q_{sat}^S$ becomes negative, then $q^S = q_{sup}^S$ is used.

- Note that the condensation and convection coefficients $\alpha$ and $h$ are both time dependent. The pressure $p(t)$ of the steam is known and the temperature $\theta_e^{sat}$ of the saturated steam is a function of the pressure. Thus the input is a table of $(t_i, p_i, \alpha_i, h_i)$ values.

- With this model, a transient analysis, preferably with full Newton equilibrium iterations, must be conducted.

- Fig. 4.3-1 shows a typical graph of surface temperature $\theta^S$ against time, distinguishing between condensation and convection heat transfers.

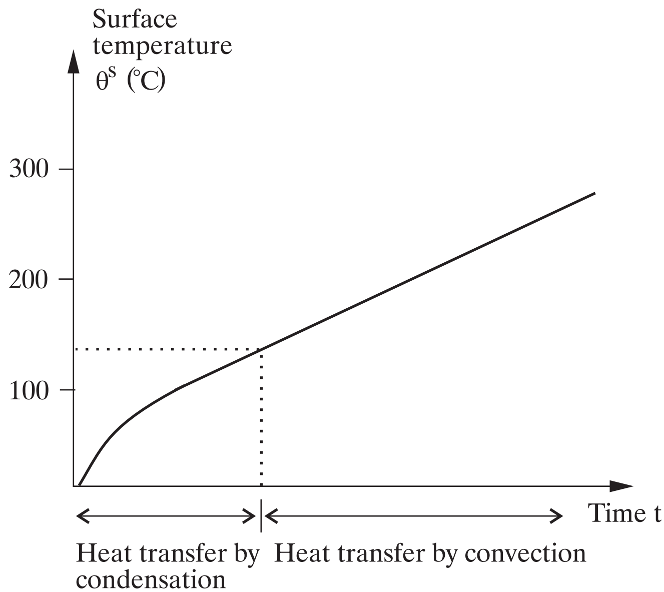


Figure 4.3-1: Typical graph of surface temperature against time for condensation/convection of body in steam

# 4.4 User supplied material model

## 4.4.1 General considerations

- The user-supplied model in ADINA-T gives you a flexible means of constructing a very general model for heat transfer analysis and for analyses of other field problems, e.g., seepage flow.

- The user-supplied model can be employed in 2-D and 3-D conduction elements, shell conduction elements and surface convection elements.

## 4.4.2 Usage of the user-supplied material model

The user-supplied material model should be included in one or more of the following subroutines:

*Subroutine TUSER2:* 2-D conduction elements, temperature-dependent properties, anisotropic conductivity matrix.

*Subroutine TUSR3T:* 3-D conduction elements, temperature-dependent properties, anisotropic conductivity matrix.

*Subroutine TUSRT7:* Shell conduction elements, temperature-dependent properties, anisotropic conductivity matrix.

*Subroutine TUSERH:* Convection elements, temperature-dependent properties.

These subroutines can be found in file at00u.f.

**The variable KEY:** The calculation process is controlled by the integer variable KEY. Element dependent variables are shown in the comments of each subroutine.

**KEY=1:** Calculation of element fluxes, based on the calculated quantities, i.e., temperature-gradients, and temperature-dependent and temperature-independent constants. In the interaction analysis with ADINA, adds contributions from solid deformations. In TUSERH, indicates calculation of surface fluxes.

**KEY=2:** Calculation of conductivity matrix, based on the calculated quantities, i.e., temperature-gradients, and temperature-dependent and temperature-independent constants. In TUSERH, indicates calculation of surface convection coefficient.

**KEY=3:** Calculation of transient properties, e.g., specific heat capacity, based on the temperature-dependent and temperature-independent constants. Not used in TUSERH.

**KEY=4:** Print out fluxes. Not used in TUSERH.

**KEY=5:** Used for consolidation analysis to provide a solid constant. Not used in TUSERH.

# 5. Boundary conditions/applied loading/constraints

From Chapter 2 we note the following types of boundary condition or loading:

- specified boundary temperatures
- specified boundary heat flux (flow)
- specified internal heat generation

We now consider each of these and how they are applied within ADINA-T.

## 5.1 Temperature

*ref. KJB Section 7.2.1*

- The boundary condition for heat transfer with a known surface temperature is given by equation (2.1-2), i.e.,

$$\theta\big|_{S_1} = \theta_e$$

where $\theta_e$ is the known temperature on some part $S_1$ of the body surface. This can be generalized to the transient case where $\theta_e$ is time dependent i.e.,

$$\theta\big|_{S_1}(t) = \theta_e(t).$$

- The simple case $\theta_e = 0$ is handled by specifying a constant zero temperature at the appropriate nodes. The more general case where $\theta_e = \theta_e(t)$ is implemented requires a time function to be defined.

- An important point to be aware of in imposing a fixed boundary temperature to an otherwise uniform body is the interpolation near the boundary for quadratic elements.

Consider a bar initially at uniform temperature $\theta_0$ with one end suddenly increased to $\theta_1$ at time $t = 0$. For linear elements the initial temperature distribution is given in Fig. 5.1-1, i.e., a linear change in temperature from $\theta_1$ to $\theta_0$ within the element adjacent to the boundary. However, for quadratic elements the parabolic interpolation functions give a temperature less than $\theta_0$ in part of the element, as shown. Conversely, a temperature greater than $\theta_0$ would result if $\theta_1 < \theta_0$.Thus, any temperature-dependent material property should allow for temperatures below (above) any physically expected minimum (maximum).

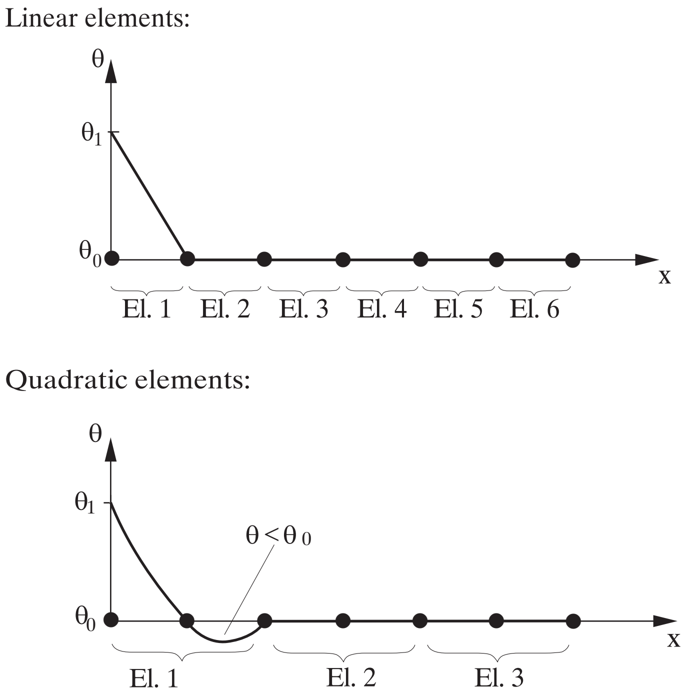


Figure 5.1-1: Interpolation of temperature boundary conditions

This observation also holds for all high order elements.

- Another temperature condition of interest is the case where a temperature at a node is linearly dependent on the temperatures at other nodes, i.e.,

$$\theta_s = \sum_{m=1}^{M} \beta_m \theta_m$$

where the "slave" node temperature $\theta_s$ depends on the "master" node temperatures $\theta_m$ according to the above equation, with $\beta_m$ being multiplicative coefficients. This includes the simplest case where

$$\theta_s = \theta_m$$

i.e., the temperature at the slave node is assumed to be identical to the temperature at the master node.

Constraints are utilized to enforce the above conditions for linearly dependent temperatures.

## 5.2 Heat flux

ref. KJB Section 7.2.1

- Applied boundary heat flux is specified by equation (2.1-3):

$$k_n \left. \frac{\partial \theta}{\partial n} \right|_{S_2} = q^S$$

where $q^S$ is the surface heat flux input to the body across some part $S_2$ of the body surface, $k_n$ is the body thermal conductivity in direction $n$, the outward normal to the surface, and $\theta$ is the temperature.

- The heat flux $q^S$ can be specified in several ways, and any combination of them is possible. First, $q^S$ may be a known, e.g., measured quantity. In this case, $q^S$ can be input either as a value distributed across an element boundary, edge or face, or as values at nodes. In each case, $q^S$ can be time- dependent, $q^S = q^S(t)$, in which case a time function should be referenced.

- The heat flux $q^S$ can be specified as a convection boundary condition where the heat flux is proportional to the temperature difference between the body surface and the external environment, i.e.,

$$q^S = h\left(\theta_e - \theta^S\right)$$

This heat flux condition is specified by the creation of convection elements (node, line, or surface as appropriate) coinciding with nodes/elements on the boundary of the domain. The material assigned to the convection elements defines the convection coefficient $h$ (constant, time- or temperature-dependent), and the environmental temperature $\theta_e$ is defined via the convection load command ($\theta_e$ can also be time-dependent).

- Another special case is that of condensation-convection, e.g., for steam environments, which is handled by a special material model for the convection elements.

- Finally, the surface flux $q^S$ can be specified as a radiation boundary condition, where the heat flux depends nonlinearly on the body surface and external radiative (source/sink) temperatures, i.e.

$$q^S = \sigma f e\left(\theta_r^4 - \left(\theta^S\right)^4\right)$$

This heat flux condition is specified by the creation of radiation elements (node, line or surface as appropriate) coinciding with nodes/elements on the boundary of the domain. The radiation elements have the property $f$ – the shape factor – assigned to them, and the material assigned to the radiation elements includes the emissivity coefficient $e$, and also the physical constant $\sigma$, the Stefan-Boltzmann constant. The radiative temperature $\theta_r$ can be time-dependent.

- For any boundary of the domain which does not have either the heat flux or temperature specified, it will be assumed by virtue of the formulation, that

$$q^S = 0$$

i.e., that this part of the boundary is "insulated," allowing no heat transfer across it.

## 5.3 Internal heat generation

*ref. KJB Section 7.2.3*

- Another form of thermal loading is given by the generation of heat within the body of the domain - i.e. within the finite elements. This is introduced into the governing equation system by the term $q^B$ of equation (2.1-1) (or $\tilde{q}^B$ (equation (2.1-5)) for transient problems). The term $q^B$ is input, for each element group, by internal heat loads where $q^B$ can be time-dependent through reference to a time function. For temperature-dependent heat generation, a temperature-dependent internal heat load must be used, whereby a table of $\left(\theta_i, q_i^B\right)$ values represents the function $q^B\left(\theta\right)$ with $\theta$ being temperature.

- The heat "generation" term $q^B$ can be negative, indicating a loss of heat within the body.

- The heat generation term can be temperature-dependent.

- Another form of heat generation comes from a change of phase from solid to liquid or vice-versa. Heat energy is involved in the molecular changes that occur during a change of phase. Thus, "latent" heat is generated or absorbed, at the interface region between the solid-liquid phases.

  The equations used can be found in the following reference:

  ref. Rolph III, W.D. and Bathe, K.J., "An Efficient Algorithm for Analysis of Nonlinear Heat Transfer with Phase Changes", *Int. J. Num. Met. Eng.*, Vol. 18, pp. 119-134, 1982.

  Several solid-liquid interfaces can be defined. The phase change temperature or temperature interval and the amount of heat energy liberated or absorbed during the phase-change transition can also be input.

- Internal heat generation is not applicable when Joule-heat analysis is present.

## 5.4 Thermostatic analysis

- ADINA-T 8.0 provides a new feature, thermostatic analysis, with the addition of the THERMOSTAT command.

- The thermostat controls the application of heat loads based on the temperature of a single sensor node or point. A cut-in and cut-off temperature specify when the associated heat loads are turned on and off respectively.

  This command can be used, for example, in an application where it is desired to predict the temperature distribution in a mold.

# 6. Radiosity

ref. KJB
Section 7.2.3

- The radiation boundary condition

$$q^S = \sigma f e\left(\theta_r^4 - \left(\theta^S\right)^4\right)$$

is employed by ADINA-T to model "gray" body radiation, via radiation elements on the domain boundary. The radiative temperature $\theta_r$ must be known, and surface interaction is modelled by the use of the shape factor (or "view" or "angle" factor) $f$.

- ADINA-T also offers a more sophisticated solution to the problem involving multiple surfaces radiating heat – each absorbing/ emitting radiation from each other.

An extra variable, the "radiosity" $R$, is defined to be the sum of the emitted energy and reflected radiation, i.e., the radiosity at a point on surface $A_1$ radiating to other surfaces $A_2$ is given by

$$R\Big|_{A_1} = e_1 \sigma \theta^4\Big|_{A_1} + \rho_1 \int_{A_2} R\Big|_{A_2} \frac{\cos\beta_1 \cos\beta_2}{\pi r^2} dA_2$$

with $\rho_1$= reflectivity = $\left(1-e_1\right)$, $\beta_1$ is the angle made between the normal to $A_1$ and the line connecting the point on $A_1$ to some other point on a surface $A_2$, $\beta_2$ is the angle made between the same line and the normal to surface $A_2$, $r$ is the length of the connecting line.

The numerical integration of the radiosity is based on the Gauss integration order. The order can be varied from 2 to 10, depending on the desired accuracy of results, but the selection of a higher integration order increases the corresponding solution time.

The definition and description of radiosity can be found in the following reference:

ref. Holman, J.P., *Heat Transfer*, 4th ed., McGraw-Hill, 1976.

- The problem is solved by introducing, in addition to the temperature degree of freedom, a nodal degree of freedom of radiosity, $R_j$, at each node of the required surfaces, i.e.,

$$R = \sum_j h_j R_j \qquad (h_j = \text{interpolation function})$$

and integrating the radiosity equation in finite element form over the radiosity surface.

- Once the radiosity is known, at all nodes, the radiative heat flux at surface $k$ is given by

$$q_k = \frac{e_k}{\rho_k}\left(\sigma\theta_k^4 - \sum_j R_j^k h_j^k\right)$$

This heat flux then enters the energy equation to solve for the temperature vector $\boldsymbol{\theta}$.

- The algorithm solves for the vectors of nodal degrees of freedom **R** and $\boldsymbol{\theta}$ simultaneously. However, the solution for **R** requires a knowledge of the surface temperature and therefore the nodal radiosities are one iteration level 'behind' the temperature. It is possible to solve for **R** alone, but the surface temperatures must be supplied.

- In ADINA-TMC, a scale factor can be applied to the radiosity heat flux terms of the tangent conductivity matrix for 2D-solid elements and 3D-solid elements using the RAD-FACT parameter of the TMC-CONTROL command. By default, RAD-FACT=1. In general, the radiosity heat flux terms of the tangent conductivity matrix are non-symmetric, however, ADINA assembles approximate (symmetrized) terms into the conductivity matrix. For most problems, the symmetrized terms improve convergence. For those problems where convergence is slowed by the symmetrized terms, or when there is no convergence, RAD-FACT=0 can be used.

- Note that the solution algorithm is derived for the "transient" analysis on the heat tranfer between surfaces, but can also be used for steady state analysis.

- The solution algorithm is derived mainly for grey diffuse radiation. A black body can be modeled, however, using an emissivity of 0.999.

**Visibility checking:** The algorithms used by ADINA-T are now summarized.

First, the program checks for a third surface (one element) obstruction by determining if a line connecting the centroids of two elements is intersected by other elements. This is done during the input phase prior to the assembly of radiosity matrices (see Fig. 6.1). Thus self-shadowing, partial self-shadowing and third surface intersecting is taken into account.

Then, during the calculation of radiosity matrices, the program verifies at the element Gauss points that

$$\mathbf{r}_{ki} \cdot \mathbf{n}_i > 0 \quad \text{and} \quad \mathbf{r}_{ik} \cdot \mathbf{n}_k > 0$$

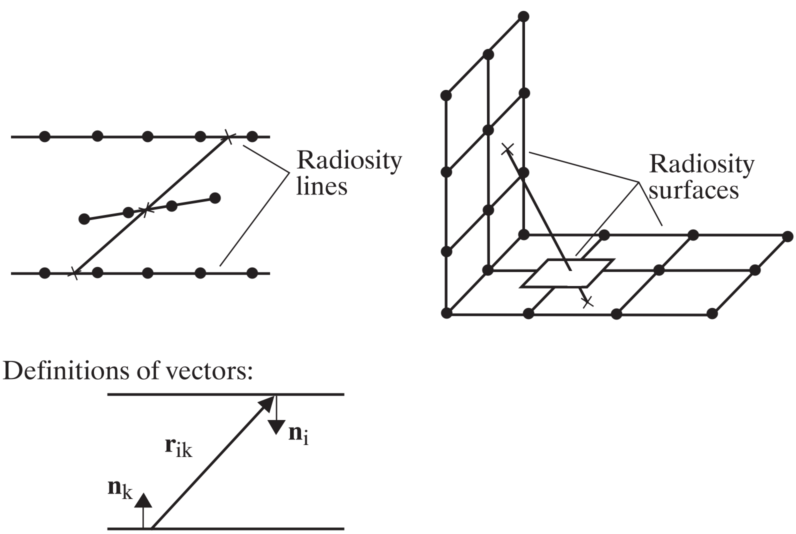


Figure 6.1-1: Visibility checks for radiosity surfaces

- Radiosity surfaces which implement the above formulation are input to ADINA-T by using 2-D radiosity surfaces (see Fig. 6.2) or 3-D radiosity surfaces (see Fig. 6.3), depending on the dimensionality of the surface.

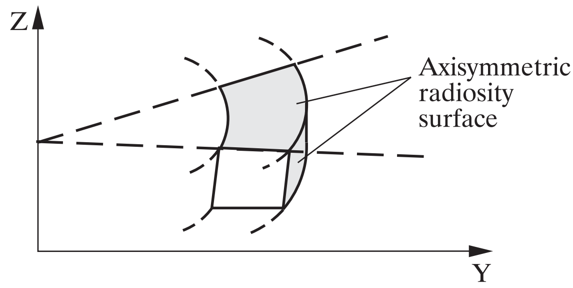


a) General axisymmetric radiation

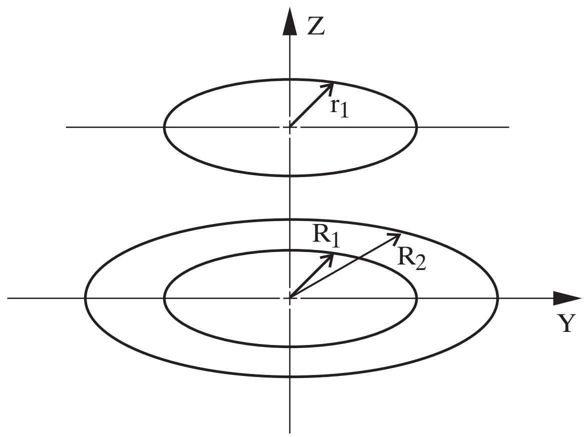


b) Parallel disk radiation

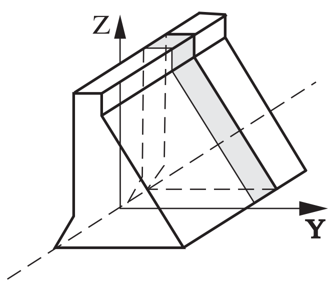


c) Planar radiosity surface

Figure 6.2: Possible 2-D radiosity surface types

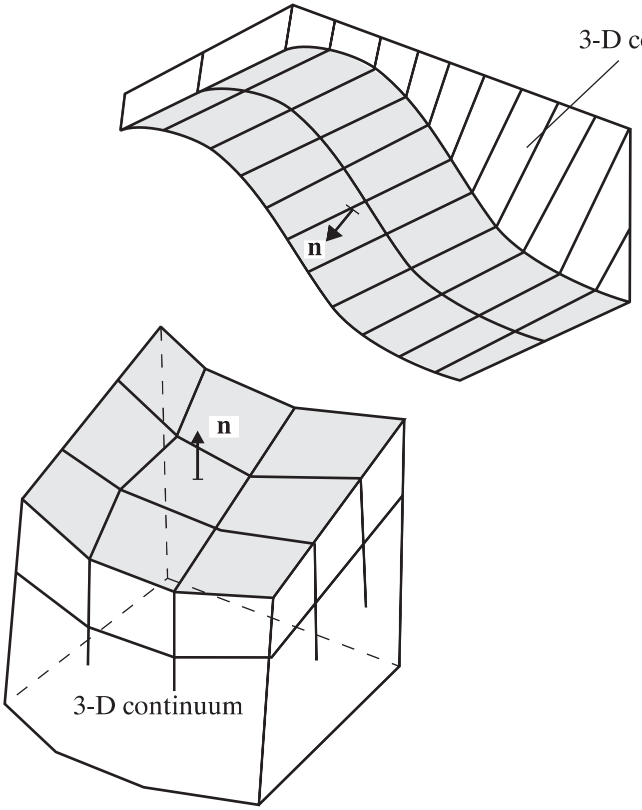


Figure 6.3: Examples of 3-D radiosity surfaces

- Transient temperatures in radiation interchange are calculated according to the flow chart in Figure 6.4, which is adapted from Figure 3.1 of the following reference:

ref. Argyris, J. and Szimmat, J., "An analysis of temperature radiation interchange problems", *Computer Meth. in Appl. Mech. and Eng*., Vol. 94, pp. 155-180, 1992

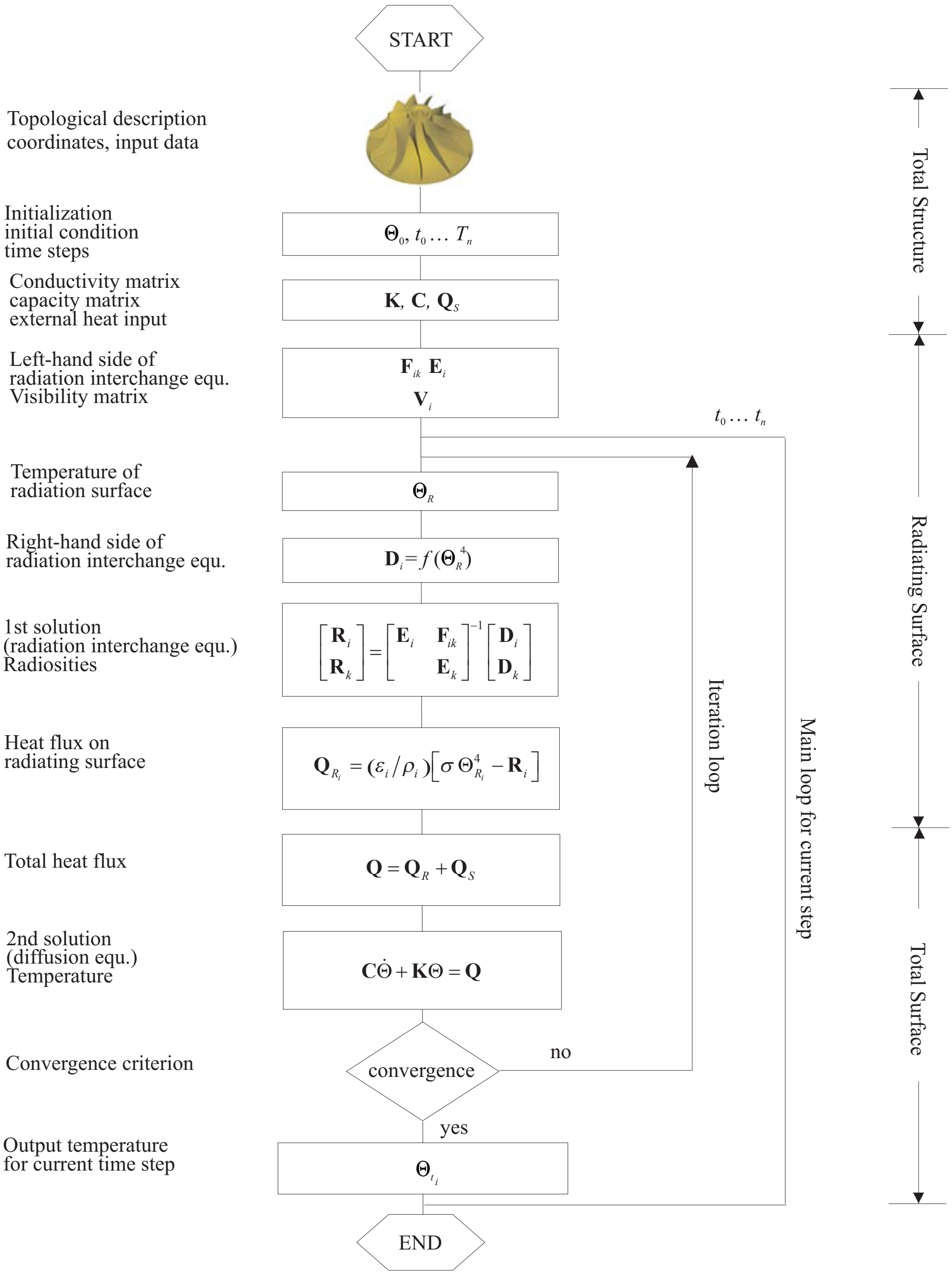


Figure 6.4: Flow chart of transient temperature calculation and radiation interchange

# 7. Solution of equation systems

## 7.1 Solution of linearized equations

### 7.1.1 Direct skyline solver

*ref. KJB Section 8.2.3*

- ADINA-T uses a direct skyline solution method with out-of-core storage.

### 7.1.2 Iterative solver

*ref. KJB Section 8.3.2*

- The iterative solution method in ADINA-T is based on the conjugate gradient algorithm with incomplete Cholesky factors as a preconditioner.

- The iterative solver should be primarily used for large systems.

- The convergence depends mainly on the structure of the matrix **A**:

$$\mathbf{A}\mathbf{x} = \mathbf{b}$$

For the above system of equations, let $\mathbf{x}_k$ be the approximate solution at iteration $k$ and the residual vector be $\mathbf{r}_k = \mathbf{b} - \mathbf{A}\mathbf{x}_k$. The criterion for convergence of the iterative solver is to satisfy either

$$\left\|\mathbf{r}_k\right\|_2 \leq \text{EPSIA} \quad \text{and} \quad \frac{\left\|\mathbf{r}_k\right\|_2}{\left\|\mathbf{b}\right\|_2} \leq \text{EPSIB}$$

or

$$\left\|\mathbf{r}_k\right\|_2 \leq \text{EPSII}$$

where

$$\text{EPSII} \leq \text{EPSIA}$$

Difficulties in convergence might be encountered when an ill-conditioned matrix **A** is used. Note, that when the iterative solver is used, only non-zero elements are stored in the **A** matrix, therefore, a substantial saving in memory/disk storage can be achieved. Also the solution times for large systems can be significantly shorter when compared with the direct skyline solver.

### 7.1.3 Sparse solver

- The sparse solver technology combines file storage savings similar to the iterative solution method with direct solution techniques. However, the memory requirement is larger than for the iterative solver, but much lower than for the skyline solver due to a sophisticated renumbering scheme. The sparse solver provides a substantial solution time reduction and can also provide good parallel scalability on some computer platforms.

The sparse solver is the default solver in ADINA-T.

## 7.2 Numerical procedures for nonlinear finite element systems

*ref. KJB Section 7.2.2*

- ADINA-T includes the modified Newton and the full Newton algorithms for solution of the incremental equations.

## 7.3 Eigensystem solution

*ref. KJB Sections 10.1 and 10.2*

- In general, the thermal equilibrium equation can be written as

$$\mathbf{C}\dot{\boldsymbol{\theta}} + \hat{\mathbf{K}}\boldsymbol{\theta} = \mathbf{Q}$$

where $\hat{\mathbf{K}}$ is the effective conductance matrix, $\mathbf{C}$ is the heat capacity matrix and $\mathbf{Q}$ is the loading term. Assuming that the temperature can be separated as follows

$$\boldsymbol{\theta} = \boldsymbol{\varphi}\, e^{-\lambda t}$$

and that there is no loading on the system $\left(\mathbf{Q} \equiv \mathbf{0}\right)$, we have

$$\hat{\mathbf{K}}\,\boldsymbol{\varphi} = \lambda\,\mathbf{C}\,\boldsymbol{\varphi}$$

This represents a generalized eigenvalue problem, i.e. $\lambda$ and $\boldsymbol{\varphi}$ are the thermal eigenvalue and eigenvector (mode shape) respectively. The complete solution can be written as

$$\hat{\mathbf{K}}\,\boldsymbol{\varphi} = \mathbf{C}\,\boldsymbol{\varphi}\boldsymbol{\Lambda}$$

where $\boldsymbol{\varphi} = \left|\boldsymbol{\varphi}_1\;\boldsymbol{\varphi}_2\ldots\boldsymbol{\varphi}_n\right|$ and $\boldsymbol{\Lambda} = \mathrm{diag}\left(\lambda_i\right)$ i.e., $\boldsymbol{\varphi}$ is a matrix of $\mathbf{C}$-orthonormalized eigenvectors.

- The stability of explicit time integration rules relates the maximum allowable timestep to the maximum eigenvalue of the system i.e.,

$$\Delta t \le \frac{\gamma}{\lambda_n} \qquad \left(\lambda_1 \le \lambda_2 \le \cdots \le \lambda_n\right)$$

where $\gamma$ is a number dependent on the element type.

However, for implicit time integration, the inherent stability of the scheme imposes no upper bound on the timestep – accuracy considerations nevertheless limit the size of $\Delta t$ which leads to acceptable solutions (see Section 7.3).

- For implicit time integration (e.g., the Euler backward method) knowledge of the lowest eigenvalues of the system provides a guide to the choice of timestep since the eigenvalue controls the rate of decay (due to the term $e^{-\lambda t}$).

- ADINA-T uses the determinant search technique to determine the eigenvalues and corresponding mode shapes.

## 7.4 Steady state analysis

- For a steady-state problem there is no heat capacity effect, i.e., the time derivative term $\dot{\theta}$ does not appear in the governing equation system. Time becomes a dummy variable which is used to indicate different load levels in an incremental load analysis.

- For incremental analysis, the loading (i.e. heat flux, temperature, boundary conditions) is applied to the model using time functions.

  The size of the load increment ("timestep") should be carefully selected. If an increment is too large the equilibrium iterations may not converge; on the other hand, too small an increment may result in many more increments being required to reach the desired load level than are necessary.

- For a steady-state analysis the temperature must be specified for at least one node in the mesh. This provides a datum level (otherwise an infinite number of solutions are possible).

## 7.5 Transient analysis

- The specific heat matrix can be lumped or consistent in a transient analysis.

- For a transient analysis, the effect of heat capacity is included in the governing equation system; thus the time derivative, $\dot{\theta}$, term appears and is integrated by the $\alpha$-method with $0 \le \alpha \le 1$ and for specific values we have

  $\alpha = 0$ – Euler forward (explicit)
  $\alpha = ½$ – trapezoidal rule (implicit)
  $\alpha = 1$ – Euler backward (implicit)

### 7.5.1 Choice of time step and mesh size

*ref. KJB Section 9.6.1*

- The choice of timestep size $\Delta t$ is important; if $\Delta t$ is too large then the system may become unstable for explicit timestepping, or in implicit integration the equilibrium iteration process may not converge for nonlinear problems. On the other hand, too small a timestep may result in extra effort unnecessarily being made to reach a given accuracy.

  Therefore it is useful to provide some guidelines as to the choice of timestep size $\Delta t$. We would like to use as large a timestep as the accuracy/stability/convergence criteria allow. Thus the guidelines are phrased as upper limits on the timestep size $\Delta t$, i.e.

$$\Delta t \le \Delta t_{\max}$$

- Consider the governing differential equation for constant thermal conductivity and heat capacity in one dimension (extrapolation to higher dimension is possible)

$$\rho c \frac{\partial \theta}{\partial t} = k \frac{\partial^2 \theta}{\partial x^2}$$

Non-dimensionalizing this equation, we use

$$\hat{\theta} = \frac{\theta - \theta_0}{q_w \, L/k} \quad ; \quad \hat{t} = \frac{t}{\tau} \quad ; \quad \hat{x} = \frac{x}{L}$$

where $\theta_0$ is the initial temperature, $\tau$ a characteristic time, $L$ a characteristic length, and $q_w$ a characteristic heat flux input. This yields the equation

$$\frac{\partial \hat{\theta}}{\partial \hat{t}} = \frac{a}{L^2} \frac{\partial^2 \hat{\theta}}{\partial \hat{x}^2}$$

where $a = \dfrac{k}{\rho c}$ is the thermal diffusivity. We take the characteristic time to be

$$\tau = \frac{L^2}{a}$$

giving the dimensionless time $\hat{t}$ and the dimensionless Fourier number $F_0$

$$F_0 = \frac{at}{L^2}$$

This number gives the ratio of the rate of heat transferred by conduction to the rate of heat stored in the medium.

To obtain a time step value, a related parameter is introduced

$$F_{0_\Delta} = \frac{a(\Delta t)}{(\Delta x)^2}$$

where $\Delta x$ is a measure of the element size. Thus, given an element size $\Delta x$ and a value of $F_0$, a timestep size can be determined. The recommended value of $F_{0_\Delta}$ given below comes from stability and accuracy considerations.

- For the Euler forward explicit time integration scheme ($\alpha = 0$) a value of

$$F_{0_\Delta} \leq \frac{1}{4}$$

or equivalently

$$\Delta t \leq \frac{(\Delta x)^2}{4a}$$

with $a = \dfrac{k}{\rho c}$ gives stable and reasonably accurate solutions (dependent on the mesh size $\Delta x$). Thus the timestep is coupled to the "element size" $\Delta x$ and the diffusivity. If low-order elements are used with explicit time integration (as is usually the case), then the element size $\Delta x$ can be taken as the minimum distance between any two adjacent corner nodes of an element (for 4-node elements in 2-D and 8-node elements in 3-D).

- For both the trapezoidal rule ($\alpha = ½$) and the Euler backward ($\alpha = 1$) implicit time integration schemes, a value of

$$F_{0_\Delta} \leq 1$$

or equivalently

$$\Delta t \le \frac{(\Delta x)^2}{a}$$

gives reasonably accurate solutions (again, overall solution accuracy depends on the "mesh size" $\Delta x$). The minimum value of $\frac{(\Delta x)^2}{a}$ over all the elements of the mesh should be employed. The "element size" $\Delta x$ is now taken, for low or high-order elements, as the minimum distance between any two adjacent corner nodes of the element.

- Thus, given a mesh size $\Delta x$, we can choose a timestep $\Delta t$ to ensure stability and accuracy (of the time integration). The question remains as to what is an acceptable mesh size $\Delta x$?

To provide guidelines for the choice of element size $\Delta x$, we consider the case of a semi-infinite solid initially at a uniform temperature, whose surface is subjected to heating (or cooling) by applying a constant temperature or constant heat-flux boundary condition.

We define a "penetration depth", $\gamma$, which represents the distance into the solid at which 99.9% of the temperature change has occurred at a time $t$. For the above posed problem, which has an analytical solution, we have

$$\gamma = 4\sqrt{at}$$

where $a$ is the thermal diffusivity. Thus the penetration zone of the domain must have a sufficient number of elements to model the spatial temperature variation, but beyond that zone larger elements can be used without loss of accuracy.

Since the penetration zone increases with time, we define a time $t_{min}$ which is the minimum 'time of interest' of the problem. $t_{min}$ may be the first time at which the temperature distribution over the domain is required, or the minimum time at which discrete temperature measurements are required.

Given this time $t_{min}$ we divide the penetration zone into a number of elements, e.g., for a one-dimensional model, such that

$$\Delta x \le \frac{4}{N}\sqrt{a t_{\min}}$$

Usually $N = 10$ gives an effective resolution of the penetration zone for a variety of boundary conditions and time integration schemes i.e.,

$$\Delta x \le \frac{2}{5}\sqrt{a t_{\min}}$$

- Please note the following:

  - For problems involving phase change, $N$ may have to be increased to maintain accuracy, e.g., $N = 20$.

  - For a given (large) $t_{min}$, the element size upper bound may be greater than the physical dimensions of the problem. In this case it is obvious that the element size must be significantly reduced.

- Although consideration was given to one-dimensional problems only, the generalization of $\Delta x$ to two- and three-dimensional problems has been shown to be valid. Hence the above element size can also be used for two- and three-dimensional problems.

### 7.5.2 Automatic time stepping method

- ADINA-T offers a user convenience in the solution of nonlinear thermal problems, when the iteration sequence fails to converge to equilibrium during a timestep (or load increment). This is the automatic-time-stepping (ATS) feature.

- Note that $\Delta t$ and $\Delta x$ must be selected as usual, that is, a timestep size $\Delta t$ is not automatically calculated, but is automatically reduced upon encountering convergence difficulties.

- Normally, when no equilibrium convergence is reached during a timestep the program terminates. With the ATS method selected, however, the timestep $\Delta t$ is automatically subdivided into smaller amounts, in an attempt to achieve convergence for each subincrement. It is assumed that applied loading varies linearly during the time $t$ to $t + \Delta t$. The maximum number of subdivisions is an input parameter.

- In addition, for transient analysis, the timestep (i.e., not load increment as in nonlinear steady-state analysis) can be automatically subdivided to achieve a more accurate solution. Subdivision is triggered when the temperature difference exceeds a certain criterion, namely

$$\max \frac{\left| {}^{t+\Delta t}\theta_i - {}^{t}\theta_i \right|}{\left| {}^{t}\theta_i \right|} \geq TEMPTOL$$

The tolerance *TEMPTOL* is an input parameter.

## 7.6 Element birth-death options

- It is possible within ADINA-T to model the removal or addition of elements in the physical system.

- The addition of elements to the system is achieved by the birth option; elements are initially inactive but at a particular solution time "$t_{birth}$" the element becomes active, i.e., contributes to the system conductivity and capacity matrices. Note: the element remains active thereafter, unless the death option later removes, or inactivates, the element.

- The removal of elements from the system is achieved by the death option; elements which are initially active (or have been activated previously by the birth option) are deactivated at a particular solution time, "$t_{death}$" - the element no longer contributes to the system conductivity or capacity matrices. Note: the element remains inactive thereafter, for all times $t > t_{death}$. Also, while it is possible for an element to be "born" and later "die", i.e.

$$t_{birth} < t_{death}$$

the converse, i.e., an element which has "died" is "born" again, is not possible in ADINA-T.

# 8. Thermo-mechanical analysis

*ref. KJB Section 7.3*

- The heat transfer and temperature analysis of a finite element model performed by ADINA-T can be used to generate temperatures for a displacement and stress analysis with ADINA.

- This chapter discusses that class of problems in which the thermal solution affects the structural solution, but the structural solution does not affect the thermal solution. See Chapter 11 for a discussion of fully coupled thermo-mechanical analysis.

- The ADINA mesh can be the same as the ADINA-T mesh, or can be different than the ADINA-T mesh.

**ADINA mesh is the same as the ADINA-T mesh**

- When the ADINA mesh is the same as the ADINA-T mesh, the temperatures calculated in ADINA-T can directly be employed in ADINA. Namely, ADINA-T stores the calculated nodal temperatures in a file which can then be used for the stress analysis. Fig. 8.1 illustrates this solution approach.

- The nodal temperatures are written by ADINA-T using the Fortran coding

```
WRITE (56) TIME,(TEMPV(I),I=1,NUMNP)
```

where

| | | |
|---|---|---|
| TIME | = | time $t$ of solution step |
| TEMPV | = | vector of nodal temperatures at time $t$ |
| NUMNP | = | number of nodal points used in ADINA-T solution |

and this same format is used by ADINA when reading the temperature file.

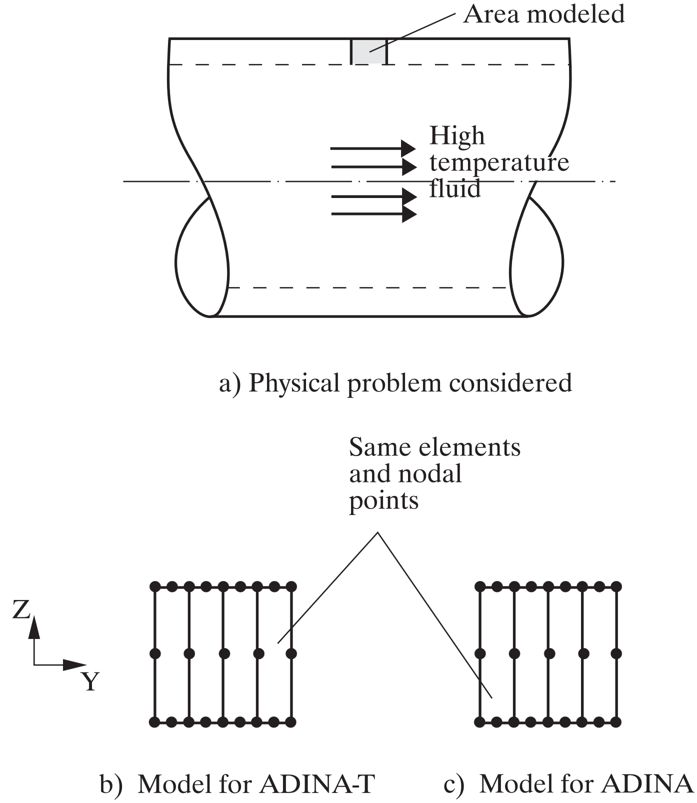


Figure 8.1: Temperature and thermal stress analysis using ADINA and ADINA-T

- The option of interpolating (in time) temperatures provided byADINA-T is available in ADINA. In this case ADINA assumes that the solution times used in the current ADINA analysis are not necessarily the same as those used in a preceding ADINA-T analysis in which the temperature file was written. ADINA establishes the required nodal temperature array for a given solution time by performing linear interpolation of temperature information available on the temperature file, see the example given in Fig. 8.2.

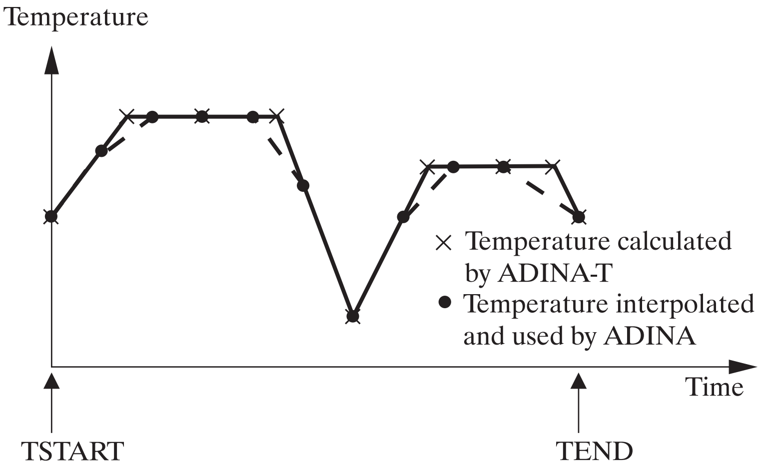


Figure 8.2: Example of temperature interpolation in ADINA using ADINA-T results

• Note that the solution time for the entire ADINA analysis must be within the range of times at which temperatures are available on the temperature file. ADINA will stop and issue an error message if

$$\text{TSTART}_{\text{ADINA-T}} \geq \text{TSTART}_{\text{ADINA}}$$

or

$$\text{TEND}_{\text{ADINA-T}} \leq \text{TEND}_{\text{ADINA}}$$

• After interpolating the temperature arrays, ADINA rewrites the temperature file using the same Fortran write statement as was used in ADINA-T, and this write statement is executed for each ADINA solution time.

Hence, if the rewritten temperature file is saved for the ADINA analysis, the interpolated temperatures will be available for reuse in future ADINA analyses.

*ref. KJB Section 7.2*

*ref. KJB Section 9.6*

• Although there is the operational advantage in using the same finite element discretization for the ADINA-T solutions, it should be noted that this solution approach may require a rather fine mesh layout for the analysis. Since the temperatures are interpolated in the same manner as the displacements, but the mechanical strains are obtained by differentiation of the displacements, it follows that the thermal strains (which are proportional to the temperatures) are in effect interpolated to a higher order than the mechanical strains. The consequence is that for coarse finite element idealizations with ADINA-T and ADINA, the stress predictions show undesirable errors (e.g., nonzero stresses, when the stresses should be zero). These errors vanish as finer finite element idealizations are employed.

Figure 8.3 summarizes the results of a simple analysis that illustrates these thoughts. The figure also indicates that an effective mesh may contain the same number of nodal points but lower-order elements for the heat transfer analysis than for the stress analysis.

- It should also be noted that when using higher-order elements, the temperatures can be significantly different within the element than at the nodal points. For example, the temperature can be negative at points within an element, although the nodal point temperatures are all positive. This observation can be important when performing an analysis (using ADINA or ADINA-T) with temperature-dependent material properties.

**ADINA mesh is different than the ADINA-T mesh**

- When the ADINA mesh is different than the ADINA-T mesh, the mapping file feature must be used to write a temperature file suitable for the ADINA model.

In this case, ADINA-T creates a mapping file containing the problem solution. The mapping file stores both the mesh information (node coordinates and element-node connectivity data) and the temperature solutions.

The AUI uses the mapping file to create a temperature file for ADINA as follows. In the model definition for ADINA, after the nodes and elements are generated, the AUI reads the mapping file. For each ADINA node, the AUI determines the temperature at that node from the mapping file using interpolation, as shown in Figure 8.4. Then when the AUI creates the ADINA data file, the AUI also creates a temperature file for the ADINA model.

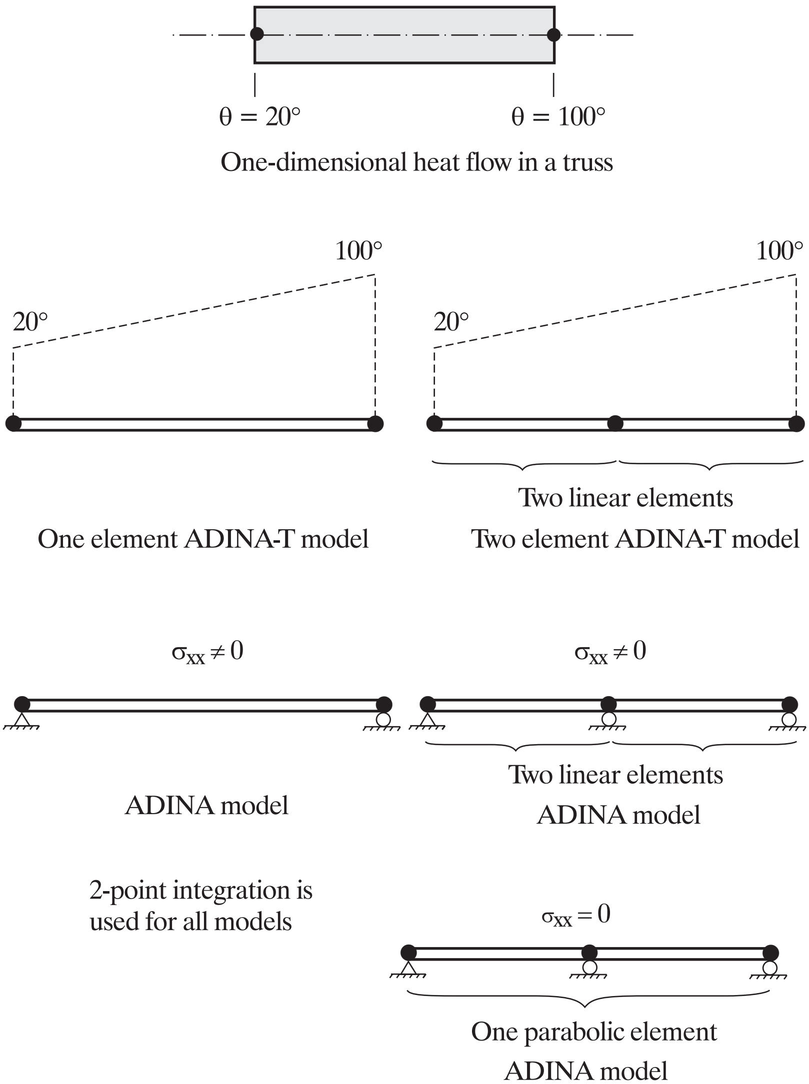


Figure 8.3: Simple problem to schematically demonstrate solution inaccuracies that can arise due to discretizations used in heat flow and stress analyses

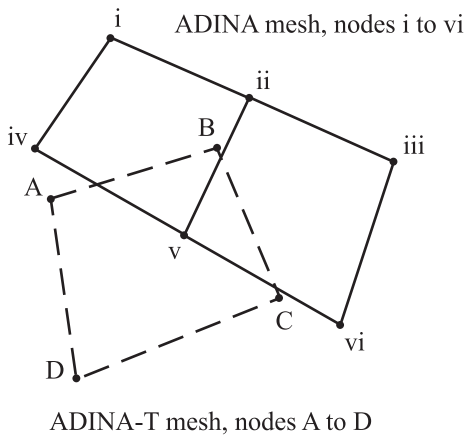


To determine the temperature at ADINA node v, the AUI performs the following steps:

The AUI locates the ADINA-T element that contains the ADINA node v.

The AUI determines the temperature at ADINA node v by interpolation from the ADINA-T nodes A, B, C.

Figure 8.4: Determining the temperature at ADINA nodes from the ADINA-T mapping file data

# 9. Soil consolidation analysis

- Coupled diffusion-stress analysis problems can be solved with the ADINA system. Such is the phenomenon of soil consolidation, in which a soil under load settles due to the dissipation of excess internal fluid pressure.

- This chapter discusses the solution of soil consolidation problems using ADINA-TMC. However, it is recommended that soil consolidation problems be solved instead using the porous media formulation of ADINA, see Section 3.12 of the ADINA Theory and Modeling Guide.

- In ADINA-TMC, the soil consolidation modeling capability is based on the linear consolidation theory, as described below.

- The soil is regarded here as a porous medium, consisting of a solid skeleton (soil particles in contact) and of interconnected voids partially or totally filled with fluid. The soil porosity, $n$, is defined as the proportion of voids per unit total volume. The void ratio, $e$, is defined as the proportion of voids to solids in any given volume. The fluid content, $\theta$, at a given fluid pressure $\pi$, is defined as the change in fluid volume, per unit total volume, between the strained state corresponding to $\pi$ and a reference unstrained state.

- The linear consolidation theory provides a macroscopic description of the soil response, based on the following assumptions:

  - The soil skeleton behavior is linear elastic isotropic.
  - The fluid is incompressible.
  - The fluid flows through the porous soil according to Darcy's law:

$$\mathbf{v} = -\mathbf{k} \cdot \nabla \pi \tag{9.1}$$

where

$\mathbf{v}$ = fluid velocity vector
$\mathbf{k}$ = soil permeability matrix
$\pi$ = fluid pressure

- Considering only small (macroscopic) strains in the soil and small velocities in the fluid, a linear stress-strain relation can be derived:

$$\boldsymbol{\sigma} = \mathbf{C}\mathbf{e} - \alpha\pi\mathbf{1} \tag{9.2}$$

where

$\boldsymbol{\sigma}$ = macroscopic stress tensor
$\mathbf{e}$ = macroscopic strain tensor
$\mathbf{C}$ = macroscopic stress-strain law matrix of the soil skeleton
$\alpha$ = first soil consolidation parameter
$\mathbf{1}$ = Kronecker delta vector

- It is also assumed that the fluid content $\theta$ varies linearly with the fluid pressure and the soil volumetric strain, i.e.

$$\theta = \alpha e_{\mathrm{v}} + \beta\pi \tag{9.3}$$

where

$e_{\mathrm{v}}$ = soil skeleton volumetric strain
$\beta$ = second soil consolidation parameter

- The general equations governing transient soil consolidation can then be established. First, the macroscopic stresses defined in equation (9.2) must satisfy the equilibrium condition:

$$\nabla \cdot \boldsymbol{\sigma} + \mathbf{f}^b = \mathbf{0} \tag{9.4}$$

where $\mathbf{f}^b$ are body forces. Second, the continuity condition for incompressible fluid flows:

$$\frac{\partial\theta}{\partial t} - q^b = -\nabla \cdot \mathbf{v} \tag{9.5}$$

where $q^b$ is the internal fluid flow generation, used together with Darcy's equation (9.1), and with equation (9.3), yields the diffusion equation controlling the variation of the fluid pressure:

$$\nabla \cdot (\mathbf{k} \cdot \nabla \pi) = \alpha \frac{\partial e_{\mathrm{v}}}{\partial t} + \beta \frac{\partial \pi}{\partial t} - q^b \tag{9.6}$$

We can now see that the stress equation (9.4) and the diffusion equation (9.6) constitute a coupled diffusion-stress equation system.

- Note on the soil consolidation parameters: From equation (9.6), it can be seen that the first soil consolidation parameter $\alpha$ is a ratio between the outward flux of fluid out of the soil and the variation in the soil volume, whereas the second soil consolidation parameter $\beta$ is a ratio between the outward flux of fluid and the variation in the fluid pressure.

- For a finite element discretization, equations (9.4) and (9.6) yield the following equation:

$$\begin{bmatrix} 0 & 0 \\ \mathbf{K}_{\pi u}^T & \mathbf{M} \end{bmatrix} \begin{bmatrix} \dfrac{\partial \mathbf{u}}{\partial t} \\ \dfrac{\partial \boldsymbol{\pi}}{\partial t} \end{bmatrix} + \begin{bmatrix} \mathbf{K}_u & \mathbf{K}_{u\pi} \\ 0 & \mathbf{K}_\pi \end{bmatrix} \begin{bmatrix} \mathbf{u} \\ \boldsymbol{\pi} \end{bmatrix} = \begin{bmatrix} \mathbf{f} \\ \mathbf{q} \end{bmatrix} \tag{9.7}$$

where

$$\mathbf{K}_u = \int_V \mathbf{B}_u^T \, \mathbf{C} \, \mathbf{B}_u \, dV$$

$$\mathbf{K}_{u\pi} = -\int_V \mathbf{B}_u^T \, \alpha \, \mathbf{H} \, dV$$

$$\mathbf{K}_{\pi u}^T = -\int_V \mathbf{H}^T \, \alpha \, \mathbf{B}_u \, dV$$

$$\mathbf{K}_\pi = \int_V \mathbf{B}_\pi^T \, \mathbf{k} \, \mathbf{B}_\pi \, dV$$

$$\mathbf{M} = \int_V \mathbf{H}^T \, \beta \, \mathbf{H} \, dV$$

$\mathbf{f}, \mathbf{q}$ = load vectors (forces, fluid flows)

$\mathbf{H}$ = interpolation matrix

$\mathbf{B}_u, \mathbf{B}_\pi$ = gradient matrices for the displacements $\mathbf{u}$ and pressure $\boldsymbol{\pi}$

- Equation (9.7) can be written as follows:

$$\mathbf{K}_u \mathbf{u} = \mathbf{f} - \mathbf{K}_{u\pi} \boldsymbol{\pi} \tag{9.8}$$

$$\mathbf{M} \frac{\partial \boldsymbol{\pi}}{\partial t} + \mathbf{K}_\pi \boldsymbol{\pi} = \mathbf{q} - \mathbf{K}_{\pi u}^T \frac{\partial \mathbf{u}}{\partial t} \tag{9.9}$$

Equation (9.8) is solved using the ADINA model, for a given fluid pressure field, and equation (9.9) is solved using the ADINA-T model, for a given displacement field. An iterative procedure can therefore be used to solve this equation system.

- The ADINA user-supplied subroutines CUSR2C and/or CUSR3C, and the ADINA-T user-supplied subroutines TUSR2C and/or TUSR3C, should be used in soil consolidation analysis. Note that, in TUSR2C and TUSR3C, KEY=5 provides the first soil consolidation parameter $\alpha$ to ADINA-T.

- Within ADINA-TMC, the ADINA and ADINA-T models are solved alternately until convergence is reached for both the structural equation (9.8) and the diffusion equation (9.9).

# 10. Piezoelectric analysis

- The solution of piezoelectric problems (direct and converse effects) can be performed with ADINA-TMC.

  Similar coupled mechanical/electrical problems including magnetostrictive, electrostrictive materials, and shape memory alloys, can also be solved with ADINA-TMC.

- In a piezoelectric material, the stresses depend on the electric potential, and the electric potential depends on the stresses. Hence, the following system must be solved:

$$\begin{bmatrix} \mathbf{K}_{UU} & \mathbf{K}_{U\Phi} \\ \mathbf{K}_{\Phi U} & \mathbf{K}_{\Phi\Phi} \end{bmatrix} \begin{bmatrix} \mathbf{U} \\ \mathbf{\Phi} \end{bmatrix} = \begin{bmatrix} \mathbf{F}_U^B + \mathbf{F}_U^S \\ \mathbf{F}_\Phi^S \end{bmatrix} \tag{10.1}$$

where

$\mathbf{K}_{UU}$ = mechanical stiffness
$\mathbf{K}_{\Phi\Phi}$ = electric permittivity matrix
$\mathbf{K}_{U\Phi}$ =piezoelectric matrix
$\mathbf{K}_{\Phi U} = \mathbf{K}_{U\Phi}^T$
$\mathbf{F}_U^B$ = body force loading vector
$\mathbf{F}_U^S$ = surface force loading vector
$\mathbf{F}_\Phi^S$ = surface charge density vector
$\mathbf{U}$ = vector of structural displacements
$\mathbf{\Phi}$ = vector of electric potentials

- For solution with ADINA-TMC, the equation system (10.1) above is written as follows:

$$\mathbf{K}_{UU}\mathbf{U} = \mathbf{F}_U^B + \mathbf{F}_U^S - \mathbf{K}_{U\Phi}\mathbf{\Phi} \tag{10.2}$$

$$\mathbf{K}_{\Phi\Phi}\mathbf{\Phi} = \mathbf{F}_\Phi^S - \mathbf{K}_{\Phi U}\mathbf{U} \tag{10.3}$$

- Equation (10.2) can be solved using the ADINA model, assuming that the electric potential field is known, and equation (10.3) can be solved using the ADINA-T model, assuming that the displacements in the structure are known.

- The ADINA user-supplied subroutines CUSR2P and/or CUSR3P, and the ADINA-T user-supplied subroutines TUSR2P and/or TUSR3P, should be used in piezoelectric analysis.

- Within ADINA-TMC, the ADINA and ADINA-T models are solved alternately until convergence is reached in both equations.

- More information about the theory and applications of piezoelectricity with the finite element method can be found in the following references:

ref. Gaudenzi P., Bathe K. J., "Recent Applications of an Iterative Finite Element Procedure for the Analysis of Electrostatic Materials," *Proceedings of the 4th International Conference on Adaptive Structures*, Nov. 2-4, Köln, Germany, 1993.

ref. Tzou H. S., Tseng C. I., "Distributed Piezoelectric Sensor/Actuator Design for Dynamic Measurement/Control of Distributed Parameter Systems: A Piezoelectric Finite Element Approach," *Journal of Sound and Vibration*, Vol. 138 (1), pp. 17-34, 1990.

# 11. Thermo-mechanical coupling

- The solution of fully coupled thermo-mechanical problems can be performed with ADINA-TMC. (In fact, TMC stands for thermo-mechanical coupling.) In this class of problems, the thermal solution can affect the structural solution and the structural solution can affect the thermal solution.

- The thermo-mechanical problems can include the following effects:

  - Internal heat generation due to plastic deformations of the material
  - Internal heat generation due to energy dissipation in a viscoelastic rubber-like material.
  - Heat transfer between contacting bodies
  - Surface heat generation due to friction on the contact surfaces.

- In this class of problems, it is necessary to alternately solve the thermal and structural models until convergence is reached. This iterative process is called “TMC equilibrium iterations”.

**Internal heat generation rate due to plastic deformations of the material:** The internal heat generation rate per unit volume due to $q_M$ is computed as

$$q_M = \omega \bar{\boldsymbol{\tau}} \cdot \bar{\mathbf{D}}^p \qquad (11.1)$$

where $\bar{\boldsymbol{\tau}}$ is the Cauchy stress tensor and $\bar{\mathbf{D}}^p$ is the plastic velocity strain tensor. The overbar denotes “corresponding to the intermediate configuration”. $\omega$ is a parameter, $0 \le \omega \le 1$, to account for possible losses.

Currently $q_M$ is computed only for 2-D and 3-D solid elements.

**Internal heat generation rate due to energy dissipation in a viscoelastic rubber-like material:** See Section 3.8.2 of the ADINA Theory and Modeling Guide for information about this material model.

**Heat transfer between contacting bodies:** With the gap conductance feature, heat transfer between closely adjacent contact surfaces can be model.

- Conductive heat transfer between closely adjacent (or contacting) surfaces is governed by an equation similar to that used for convection boundary conditions. The heat flux entering contact surface $I$ is

$$q_c^I = \omega \hat{h} \left( \theta^J - \theta^I \right) \tag{11.2}$$

where $\omega$ is the gap conductance, $0 \le \omega \le 1$, $\hat{h}$ is the contact heat transfer coefficient, and $\theta^I$ and $\theta^J$ are the temperatures of the contacting surfaces.

- Note that in the limit as $\hat{h}$ approaches infinity, the temperatures of the contacting surfaces become equal to each other. With $\hat{h}$ large, Eq. (11.2) can be considered to be a penalty method approximation to the equation $\theta^I = \theta^J$.

- The gap conductance $\omega$ controls the amount of heat transfer. It can be used to simulate conductive (and convective) heat transfer that might occur in the clearance gap before contact. In addition, gap conductance can significantly improve the convergence rate as it smoothes the discontinuity in heat conductance at initial contact.

- The following gap conductance options are available:
  - ▸ *Clearance (gap) option:* The gap conductance $\omega$ is a function of the clearance gap, $g$ only.
  - ▸ *Contact Pressure Option:* The gap conductance $\omega$ is a function of the contact pressure, $p$ only.
  - ▸ *Clearance-Pressure Option:* The gap conductance $\omega$ is a function of the clearance gap, $g$, before contact is established, and is a function of the contact pressure, $p$, after initial contact.

  *Time function option:* The gap conductance $\omega$ is govern by a time function starting with an initial contact.

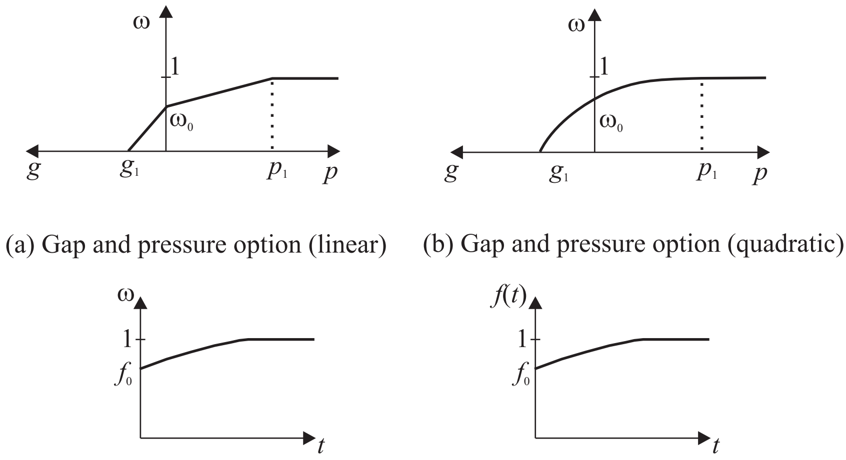


(a) Gap and pressure option (linear) (b) Gap and pressure option (quadratic)

(c) Time function option (d) Time function used in (c)

Figure 11-1: Options used to define the gap conductance, ω

- In the clearance-pressure option, the critical clearance gap and critical contact pressure, $g_1$ and $p_1$, respectively, must be defined. There is no heat conductance between the surfaces when $g \geq g_1$, and there is full heat conductance when $p \geq p_1$; see Fig. 11-1(a). Also, the gap conductance, $\omega_0$, at initial contact (i.e. when $g = 0$ and $p = 0$) must defined. Hence,

$$
\begin{aligned}
&g \geq g_1; && q_c^I = 0 \\
&g = 0 \text{ and } p = 0; && q_c^I = \omega_0\, \hat{h}\left(\theta^J - \theta^I\right) \\
&p \geq p_1; && q_c^I = \hat{h}\left(\theta^J - \theta^I\right)
\end{aligned}
$$

- In the time function option, the time function, $f(t)$, specifies the gap conductance after initial contact. Arrival times are automatically set for every contact node once the node is in a contact state. If the node status becomes out-of-contact, then the time function is set to zero. If the node becomes again in contact, then a new arrival time is set for the time function.

The gap conductance time function must cover the full solution time.

- The gap conductance is defined using the GAP-CONDUCTANCE command. The default gap conductance for a contact group can be specified using the GAPC-NAME parameter of the CGROUP command, and the gap conductance for inidividual contact pairs can also be specified using the GAPC-NAME parameter of the CONTACTPAIR command.

**Surface heat generation rate due to friction:** The frictional contact heat generation rate at a contactor node $G$ is computed as

$$q_G^{IJ} = \tau \cdot \dot{\mathbf{U}} \tag{11.3}$$

where $\tau$ is the frictional contact force and $\dot{\mathbf{U}}$ is the relative velocity between the contacting bodies at the point of contact.

The heat rate going to the contactor body is $f_c q_G^{IJ}$ and the heat rate going to the target body is $f_t q_G^{IJ}$, where $f_c$ and $f_t$ are parameters to account for possible losses. The following relations must hold:

$$0 \le f_c \le 1, \qquad 0 \le f_t \le 1, \qquad 0 \le f_c + f_t \le 1$$

The contactor heat rate is applied to the contactor node. The target heat rate is distributed among the target segment nodes. The parameters $\hat{h}$, $f_c$, $f_t$ can be specified for the whole contact group, or for each contact pair.

**Solution procedure:** ADINA-TMC is employed to obtain the solution. At the beginning of each time step, the ADINA model is solved for the displacements using the current temperatures. Then the ADINA-T model is solved for the temperatures using the current displacements. If TMC iterations are not required, the algorithm proceeds to the next time step. Otherwise the ADINA and ADINA-T models are solved using the new current displacements and new current temperatures until convergence in displacements and temperatures is reached.

- The same convergence parameter is used in the displacement and temperature convergence checks.

- Using a staggered approach, it may be advantageous to proceed without TMC iterations. Of course, then it is necessary to use a small enough time step to obtain an accurate solution.

**Further information:** More information about TMC analyses can be found in the following reference:

ref. D. Pantuso, K.J. Bathe, P.A. Bouzinov, "A finite element procedure for the analysis of thermo-mechanical solids in contact", *Computers and Structures*, Vol 75, #6, 551-573, 2000.

- Only 2-D and 3-D solid elements of ADINA and corresponding 2-D conduction and 3-D conduction elements of ADINA-T can be used in TMC analysis.

- There should be no constant global heat capacity and conductivity matrices in the ADINA-T model. To ensure this, the element groups in the ADINA-T model must be nonlinear element groups.

- Materials used in the ADINA model must be temperature-dependent.

This page intentionally left blank

# 12. Joule-heat analysis

- In a Joule-heat analysis, the temperature distribution is computed using the usual heat transfer equation (Eq. 2.1-1), except that the heat generation term includes the effects of Joule heating:

$$q^B = \left(q^B\right)' + \int J\, dE \qquad (12.1\text{-}1)$$

where $\left(q^B\right)'$ includes heat capacity and other possible heat generation terms, $J = \sigma E$ is the current density, $E = \nabla V$ , and $V$ is the electrical potential. Also $\sigma$ is the electrical conductivity.

- The electrical field distribution is computed using the Laplace equation

$$\nabla \cdot \sigma \nabla V = 0 \qquad (12.1\text{-}2)$$

- The solution is obtained in two phases:

  ▸ In phase I, we solve (12.1-2) with a steady-state analysis. The boundary conditions can be prescribed voltages and/or applied current densities on lines and surfaces.

  ▸ In phase II, we solve (12.1-1) with either a steady-state or transient analysis, in which the Joule heating effect is included in the heat generation term.

- As usual, the temperatures and heat fluxes are stored in the porthole file for post-processing, and the temperatures are stored in the temperature file for thermal stress analysis. The electrical potential and current densities are also stored in the porthole file for post-processing.

- Electric flow and heat transfer between bodies in contact can be modeled in ADINA-TMC. In the TMC analysis, the element groups in the ADINA-T model must be nonlinear element groups, see Chapter 11 on Thermo-Mechanical Coupling, in particular p. 79. Typical applications where this feature is used are the modeling of electric contact switches and electric resistance welding.

- Internal heat generation cannot be used in Joule-heat analysis.

- Using a Joule-heat analysis, you can use ADINA-T to study the effects of current density and temperature distributions on radio-frequency cardiac ablation.

  ref. Panescu *et. al.*, "Three-Dimensional Finite Element Analysis of Current Density and Temperature Distributions During Radio-Frequency Ablation", *IEEE Transactions on Biomedical Engineering*, Vol. 42, No. 9, pp. 879-889, September 1995.

# Index

## G



## H



## I



## M



## O



## P



## R



## S



## T

## U